CHARACTERISATION OF METABOLIC AND MITOCHONDRIAL DYSFUNCTION IN THE ISOPROTERENOL MODEL OF HEART FAILURE: THE ROLE OF METFORMIN

Vernice Roxanne Peterson

Dissertation submitted to the Faculty of Health Sciences, University of the Witwatersrand, Johannesburg, in fulfillment of the requirements for the degree of Master of Science in Medicine

Johannesburg, 2013

DECLARATION

I, Vernice Roxanne Peterson, declare that this dissertation is my own work. This dissertation is being submitted for the degree of Master of Science in Medicine in the Faculty of Health Science at the University of the Witwatersrand, Johannesburg, South Africa. I declare that the dissertation submitted is entirely my own, original work and the copy right of this dissertation rest with the author or the University to which it was submitted. The work herein has not been submitted before for any degree or examination at this or any other University.

Vemice Roxanne Peterson

Signed on the 5th day of February 2013

Thanking all my loved ones and mentors for their support through this endeavor. Without your patience, guidance and support this would have not been possible.

CONFERENCE PRESENTATIONS ARISING FROM THIS STUDY

The following oral presentations were offered in support of this dissertation:

Vernice R Peterson, Michael Madziva, Gavin Norton and Siyanda Makaula. Metformin modulates Cardiac Function in Isoproterenol model of Heart Failure in Sprague-Dawely Rats. 39th Congress of the Physiological Society of Southern Africa (PSSA), held at the University of Western Cape, Cape Town, 29-31 August 2011.

Vernice R Peterson, Michael Madziva, Gavin Norton and Siyanda Makaula. Metformin modulates Cardiac Function in Isoproterenol model of Heart Failure in Sprague-Dawely Rats. University of the Witwatersrand, Faculty of Health Science, Biennial Research Day and Postgraduate Expo, held on 19 September 2012.

ABSTRACT

Heart failure is a devastating disease which despite significant advances in therapy over the past two decades still results in a poor prognosis. Metabolic dysregulation is associated with heart failure; however, it remains unclear whether isoproterenol exerts deleterious effects through altered metabolic regulation. Whether metformin, a metabolic modulator, prevents isoproterenol-induced heart failure is unknown. The aim of this study was to determine whether metformin prevents functional and metabolic changes seen in the isoproterenol model of heart failure. Male Sprague-Dawley rats were administered isoproterenol and metformin for seven months. Thereafter, cardiac dimensions, metabolic gene expression and myocardial structural changes were assessed. Chronic administration of isoproterenol induced left ventricular dilatation and pump dysfunction and mitochondrial structural derangement. No changes were seen in metabolic gene expression. However, co-administration of metformin prevented isoproterenol-induced heart failure and retained mitochondrial structural arrangement. Therefore, cardiac dilatation and pump dysfunction induced by chronic administration of isoproterenol can be prevented by co-administering metformin.

ACKNOWLEDGEMENTS

I would like to extent gratitude to the following individuals who have assisted me through the course of my MSc research:

Dr Siyanda Makaula: for your scientific input, guidance and financial support.

Dr Michael Madziva: for your guidance, moral support and technical assistance in cell culture and molecular aspects of the study.

Central Animal Service: I am truly grateful to the staff of the Central Animal Service for the housing and upkeep of my 'babies'. The pleasant atmosphere and friendly smiles will never be forgotten.

Prof. Gavin Norton: For your scientific input, moral support, patience and guidance throughout the study and write-up process of this thesis. Thank you, also, for performing echocardiography on all the rats and for the financial support.

Ms Margaret Badenhorst: For your nurturing, mothering nature. I am grateful to have worked many hours with you optimizing kits and preparing sections for Transmission Electron Microscopy. The hours we spent in the laboratory will be cherished as the guidance, friendship and support has been invaluable. Also, I will never forget your refreshing and enthusiastic statement: "I TOLD YOU SO."

Mrs Pamela Sharp and the Microscopy and Microanalysis Unit: For your expertise in Transmission Electron Microscopy, developing all those micrographs and individually packaging them and the invaluable friendly assistance.

Prof Kennedy Erlwanger and Dr Richard Brooksbank: For your technical assistance with fasting blood substrates and real-time PCR skills.

Mr Andrew Raymond: For always going the extra mile in assisting me. Your laboratory assistance and company have been invaluable.

Mr Zwelibi Majola: For assisting in the termination of the animals and the collection of the tibia.

Mr Justin Hean: For your assistance with the spectrophotometer.

Financial Support: To the Medical Faculty Research Endowment Fund and the Iris Hodges Cardiovascular Research Grant of the University of the Witwatersrand, the National Research Foundation (NRF) and NRF Thuthuka Research Grant of South Africa, Carnegie Large Research Grant, Cardiovascular Pathophysiology and Genomics Research Unit (CPGRU) and the School of Physiology, without their financial support this research would have not been possible.

My Parents: for giving me the foundation which allowed me to achieve my dreams. Thank you for the guidance, support and encouragement throughout this journey.

TABLE OF CONTENTS

Page

LIST OF FIGURES

LIST OF TABLES

LIST OF ABBREVIATIONS

AMP	Adenosine 5'-monophosphate protein
AMPK	Adenosine 5'-monophosphate protein kinase
AMPKα2	Adenosine 5'-monophosphate protein kinase alpha 2
ANOVA	Analysis of variance
ATP	Adenosine triphosphate
cDNA	Complementary deoxyribonucleic acid
CONT	Control vehicle
ED PWT	End-diastolic posterior wall thickness
ES PWT	End-systolic posterior wall thickness
FS_{end}	Endocardial fractional shortening
FS_{mid}	Midwall fractional shortening
g	Gram
GAPDH	Glyceraldehyde-3-phosphate dehydrogenase
ISO	Isoproterenol
ISO+MET	Isoproterenol and metformin
KCl	Potassium chloride
KH_2PO_4	Monobasic potassium phosphate
LV	Left ventricle\ventricular
LVEDD	Left ventricular end-diastolic internal diameter
LVESD	Left ventricular end-systolic internal diameter
LVEDD PWT	Left ventricular end-diastolic internal diameter posterior wall thickness
LVESD PWT	Left ventricular end-systolic internal diameter posterior wall thickness
LVH	Left ventricular hypertrophy

LVM	Left ventricular mass
LVM/TL	Left ventricular mass adjusted for tibial length
MET	Metformin
mg	Milligram
ml	Millilitre
mmol	Millimole
mRNA	Messenger ribonucleic acid
NaCl	Sodium chloride
$Na_2HPO_4.7H_2O$	Dibasic sodium phosphate, 7-hydrate
NaOH	Sodium hydroxide
NRF-1	Nuclear respiratory factor-1
NS	Not significant
PBS	Phosphate buffered saline
PGC-1α	Peroxisome proliferator-activated receptor gamma co-activator 1-alpha
RAAS	Renin angiotensin aldosterone system
RNA	Ribonucleic acid
ROS	Reactive oxygen species
RT-PCR	Real-time polymerase chain reaction
SEM	Standard error of the mean
SNS	Sympathetic nervous system
Tfam	Mitochondrial transcription factor A
TG	Triglyceride
TL	Tibial length
µl	Microlitre
x g	Gravitational force

Chapter 1

Introduction

1.1. Determinants of Heart Failure

Heart failure is defined as the inability of the cardiac pump to meet the energy requirements and haemodynamic demands of the body (Ventura-Clapier *et al*., 2003; Gundewar *et al*., 2009). Heart failure is no longer considered to be a simple contractile haemodynamic disorder or disease, but instead, the inclusion of cellular and molecular components in maintaining homeostasis have become more prominent (Packer, 1992; Cohn *et al*., 2000). These cellular and molecular changes will be described in more detail under the adaptations of heart failure. The most common clinical characteristics of heart failure include increase in heart size, alteration of shape and deterioration of cardiac function (Cohn *et al*., 2000; Kemp & Conte, 2012). Consequently the characteristics are manifestations of major pathogenic factors, which include defects in bioenergetics, increased haemodynamic preload and after-load, altered signaling pathways as well as neurohormonal dysregulation (Packer, 1992; Cohn *et al*., 2000; Goffart *et al*., 2004; Rosca & Hoppel, 2010). These factors all contribute to development of cardiac remodeling which can be seen with an increase in heart size known as hypertrophy and in heart failure. Cardiac hypertrophy is a compensatory response that occurs when the heart is subjected to sustained increases in functional load or stress thus allowing the heart to maintain cardiac demand (Badeer, 1964; Rimbaud *et al*., 2009). It is accompanied by both structural and metabolic remodeling. Structural remodeling is characterised by increased diameter and length of the cardiac sarcomere fibers and subsequent increase in heart mass whereas metabolic remodeling is characterised by a switch in metabolic substrate preference.

1.2. Heart Failure and the Presence of Cardiac Remodeling

The most important causes of heart failure originate from coronary artery disease; acute myocardial infarction and pressure overload (hypertension) (Ventura-Clapier *et al*., 2003; Gundewar *et al*., 2009, Wang *et al*., 2011). Gundewar and colleagues (2009) have reported that the presence of these diseases lead to loss of function in cardiac myocytes, myocardial fibrosis and left ventricular remodeling, thus ultimately leading to the development of left ventricular dysfunction. Left ventricular remodeling is a deleterious process that compromises the heart and is a major component involved in the development of heart failure (Teerlink *et al*.,1994).

Characteristic of heart failure is an increase in left ventricular mass, thinning of the left ventricular wall, elevated left ventricular end-diastolic pressure and increased systemic vascular resistance, thus affecting the heart's ability to function efficiently (Stanley & Chandler, 2002; Fukuta & Little, 2007). Heart disease as a result of hypertension is characterised early by the development of pathologic left ventricular hypertrophy (LVH). Signs of ventricular enlargement and dysfunction may be present in pathological LVH (de las Fuentes *et al*., 2002). Studies have shown that the presence of eccentric or concentric hypertrophy in the heart will predict the form of heart failure present (Badeer, 1964; Fukuta & Little, 2007), and by measuring the degree of remodeling the prognosis of heart failure can be determined (Cohn et al., 2000).

The use of echocardiography is a standard technique used in animal models and clinically to determine LVH and pump dysfunction (Grimm *et al*., 1998; Gibbs *et al*., 2004; Osadchii *et al*., 2007; Stewart *et al*., 2008; Gundewar *et al*., 2009; Benes *et al*., 2011; Chen *et al*., 2011;

Yin *et al*., 2011; Booysen *et al*., 2012; Cittadini *et al*., 2012). Remodeling of the left ventricle is evident in most studies investigating hypertrophy and the progression to heart failure in animal models therefore it is of utmost importance to understand the general pathophysiological mechanisms which are activated in the various models.

1.3. Animal Models used to induce Heart Failure

Cardiac remodeling is evident in most studies that involve animal models of hypertrophy and the progression to heart failure. Many studies have investigated heart failure in the animal model through aortic banding or constriction and pacing, which induce pressure overload (Norton *et al*., 2002; Garnier *et al*., 2003; Bugger *et al*., 2010; Dunn *et al*., 2011). Alternatively, β-adrenergic stimulation and aorto-caval fistula which induce volume overload have also been used (Nagano *et al*., 1992; Murad & Tucci, 2000; Taimor *et al*., 2001; Osadchii *et al*., 2006; Osadchii *et al*., 2007; Kralova *et al*., 2008; Melenovsky *et al*., 2011). Table 1.1 lists examples of studies that have investigated various models of hypertrophy and heart failure. The table shows pressure-overload, volume-overload and neurohormonal activation animal models and highlights the key findings observed in the listed studies. These findings will be explained in more detail in the relevant sections of the introduction. Although the studies have been listed according to study duration, the most commonly observed pathological defect is LVH and pump dysfunction with the exception of a few studies which have reported biventricular hypertrophy. Biventricular hypertrophy is hypertrophy of both the right and left ventricle.

Table 1.1 Summary of selected studies involving animal models of hypertrophy and heart failure and the pathologies observed.

Reference	Species/ Strain	Model	Study Duration	Pathologies Observed
Nagano *et al*., 1992	Wistar rats	β-adrenergic induced	7 days	Increase in heart rate, LVH, increase in plasma Angiotensin II
Davel *et al*., 2008	Mice	β-adrenergic induced	7 days	LVH, Gene and protein expression of IL-1β, IL-6 and increased oxidative stress
Heather *et al*., 2009	Wistar rats	β-adrenergic induced	7 days	LVH, dilation, fibrosis, pump dysfunction, downregulation of fatty acid metabolism, decrease in GLUT4 levels
Larkin *et al*., 2004	Mice	Angiotensin II induced	14 days	Elevated blood pressure (acute), Myocardium hypertrophy, oxidative stress response, downregulation of energy pathways
Dunn *et al*., 2011	Mice	Pressure overload	3 & 6 weeks	LVH, derangement of cardiac ultrastructure, function and metabolism
Liu *et al*., 1991	SD (♀)	Volume overload	1 week & 1 month	Biventricular myocyte hypertrophy, right ventricular pressure increased
Osadchii *et al*., 2007	SD	β-adrenergic induced	3 months	LVH, LV dilatation and pump dysfunction, apoptosis, downregulation of contractility
Melenovsky *et al*., 2011	Wistar rats	Volume overload	3 months	Biventricular myocyte hypertrophy, downregulated mitochondrial metabolic pathways, altered fatty acid metabolism
Bugger et al., 2010	SD	Pressure overload	5 months	Pump dysfunction, reduced ejection fraction, mitochondrial ultrastructure derangement, reduced fatty acid & glucose oxidation, respiratory dysfunction
Gibbs *et al*., 2004	SHR & WKY rats	β-adrenergic induced	7 months	Increase in LV cavity dimension, pump dysfunction, increase in myocardial collagen cross-link

Abbreviations: GLUT4 = Glucose transporter 4; LVH = left ventricular hypertrophy; LV = left ventricular; LVESD = left ventricular end-systolic diameter; LVEDD = left ventricular end-diastolic diameter; SD = Sprague Dawley; SHR = spontaneously hypertensive rats; WKY = Wistar Kyoto rats.

In all models of heart failure the activation of β-adrenergic receptor stimulation is present and serves as a homeostatic response to cardiac stress. The sympathetic nervous system plays an important role in the adaptation of the heart to various stressors and through the activation of β-adrenergic receptors increases in heart rate, relaxation speed and contractility result in an adaptive response (Andersson *et al*., 2011; Bernstein *et al*., 2011). An increase in adrenergic activity causes tachycardia, cutaneous vasoconstriction and reduced urinary output; these are just a few factors involved in preserving circulatory homeostasis in severe heart failure (Packer, 1988; Braunwald, 2001).

The renin-angiotensin-aldosterone system (RAAS) and the sympathetic nervous system (SNS) are activated in the event of a decrease in myocardial function, which is present in heart failure, thus maintaining adequate efficiency of the heart (Tuunanen & Knuuti, 2011). Heart failure is associated with metabolic changes that are caused by hyperadrenergic effects, that is an increase in circulating free fatty acids, impaired glucose metabolism, hyperglycaemia and insulin resistance (Watson *et al*., 2006; Opie & Knuuti, 2009). The activation of RAAS can be found in patients with heart failure and leads to the formation of angiotensin II (ANG II) which is a major cause of hypertension (Francis *et al*., 1990; Larkin *et al*., 2004). The increase in ANG II and hormones in heart failure lead to activation of SNS and these induce an increase in blood pressure. However, if the activation of β-adrenergic receptors is prolonged the blood pressure will return to normal but myocardial cell damage will result (Larkin *et al*., 2004).

A study which investigated metabolic characterisation of volume overload heart failure due to aorto-caval fistula in rats for 3 months reported biventricular myocyte hypertrophy, increased

circulating free fatty acids with decreased intramyocardial triglycerides, reduced response to insulin and depletion of intraabdominal adipose tissue (Melenovsky *et al*., 2011). In response to aorto-caval fistula-induced volume overload, the activation of the neurohumoral systems RAAS and SNS ensues; as a result of sustained decrease in mean arterial pressure and the placement of the fistula (Abassi *et al*., 2011). However, as seen in Table 1.1 the pathological defects of the volume overload models are similar in that the studies both reported biventricular hypertrophy compared to the β-adrenergic and pressure overload models.

Table 1.2 is a summary of animal studies which have investigated the effects of acute and chronic isoproterenol administration and the pathological defects. Although there are a few differences between the studies with regards to dose and duration the common characteristic found in both acute and chronic isoproterenol administration is the presence of cardiac hypertrophy. Also the studies which investigated chronic administration all showed LVH with cardiac dilatation and pump dysfunction (Grimm *et al*., 1998; Gibbs *et al*. 2004; Osadchii *et al*., 2007; Booysen *et al*., 2012), indicating that acute and chronic isoproterenol models are reliable models to reproduce hypertrophy and cardiac dilatation and pump dysfunction. Left ventricular remodeling differs between the volume overload model when compared to both the pressure overload model and adrenergic model. Although SNS activation is a common characteristic amongst all models the outcomes have different end points with regards to metabolism, gene expression and mitochondrial function and ultrastructure architecture.

Table 1.2 Summary of animal studies investigating either acute or chronic isoproterenol administration and the observed pathologies.

Reference	Species/ Strain	Administered Dose & Route	Study Duration	Pathological Defect
Leenen *et al*., 2001	Wistar rats	4.2mg/kg/day, s.c	2 & 7 days	Reduced BP, increased HR, cardiac hypertrophy, increase plasma rennin activity
Nagano et al., 1992	Wistar rats	4.2mg/kg/day	7 days	Increase in heart rate, LVH, increase in plasma Angiotensin II
Zarrinpashneh *et al*., 2008	Mice	50mg/kg/day, i.p	7 days	LVH, AMPK activity remained unchanged
Davel *et al*., 2008	Mice	0.3mg/kg/day, s.c	7 days	LVH, Gene and protein expression of IL-1β, IL-6 and increased oxidative stress
Mikusova *et al*., 2009	Wistar rats	5mg/kg/day, s.c	7 days	Cardiac hypertrophy, architectural changes in cardiomyocyte ultrastructure
Heather *et al*., 2009	Wistar rats	0.5 mg/kg/day, s.c	7 days	LVH, dilation, fibrosis, pump dysfunction, downregulation of fatty acid metabolism, decrease in GLUT4 levels
Cha et al., 2010	Mice	15mg/kg/day, s.c	1 week	Cardiac hypertrophy, no change in AMPK activity
Grimm *et al*., 1998	SD (♀)	150mg/kg/day, s.c	2 &16 weeks	LV dilatation and hypertrophy. 2 weeks: elevation in plasma renin activity, aldosterone and ACE
Osadchii *et al*., 2007	SD	0.1mg/kg/day, i.p	3 months	LVH, LV dilatation and pump dysfunction, apoptosis, downregulation of contractility
Booysen *et al*., 2012	SD	0.01mg/kg/day, i.p	6 months	LVH, cardiac dilatation, pump dysfunction, contractile disturbances
Gibbs *et al*., 2004	SHR & WKY rats	0.02mg/kg/day, i.p	7 months	Increase in LV cavity dimension, pump dysfunction, increase in myocardial collagen cross-link

Abbreviations: AMPK = adenosine 5' monophosphate protein kinase; GLUT4 = glucose transporter 4; LVH = left ventricular hypertrophy; SD = Sprague Dawley rats; SHR = spontaneously hypertensive rats; WKY = Wistar Kyoto rats

Cardiac remodeling is an important variable as it is present in all models of heart failure and has now become an important target for therapeutic drug development (Cohn *et al*., 2000). As there are various models of heart failure, not all therapies available are effective (Packer, 1992). Previously, the treatment of heart failure was tailored to correct haemodynamic derangement. In heart failure, failure of the myocardium to contract and relax is accompanied by neurohumoral activity (Opie & Knuuti, 2009). The therapeutic drugs, angiotensin-converting enzyme (ACE) inhibitors and beta-blockers, have been the most successful drug therapies for treating heart failure (Rosca & Hoppel, 2010; Opie & Knuuti, 2009). The development of the neurohormonal model of heart failure assists in understanding the physiological abnormalities that remain even after symptom relief though the administration of beta-blockers (Packer, 1995). Beta-blockade decreases free fatty acid uptake in the myocardium and therefore increases work efficiency in heart failure (Opie & Knuuti, 2009). However, it is unknown whether administration of metabolic drug therapy, such as the administration of metformin, would also assist in reducing morbidity and mortality in patients with heart failure.

1.4 Cardiac Energy Metabolism in the Normal and Hypertrophied Heart

The heart requires a continuous supply of ATP therefore the adult cardiomyocytes in the normal functioning heart have a high density of mitochondria which provide an increased amount of energy to meet the high energy demand of the heart (Goffart *et al*., 2004; Iglewski *et al*., 2010). Mitochondria contain two layers, the outer layer which serves as a barrier for

protein greater than 5000 Daltons in size and the inner layer which is impermeable membrane contains multiproteins that are involved in the electron transport chain (Iglewski *et al*., 2001). In the normal functioning adult heart, fatty acids are the main source of energy and approximately 60-70% of the ATP is derived from mitochondrial fatty acid oxidative phosphorylation (Ashrafian *et al*., 2007). While fatty acid oxidation yields more ATP, fatty acid generation requires more ATP and higher oxygen consumption and therefore further increases metabolic demand in the energy-demanding hypertrophied heart. However, when cardiac hypertrophy occurs, in the compensatory stages of heart failure, energy utilisation is switched therefore glucose is the preferred metabolic energy substrate and glycolysis is increased (Leong *et al*., 2002; Jullig *et al*., 2008). Glucose metabolism is selected as a compensatory energy source as opposed to fatty acid oxidation that occurs in the normal functioning adult heart. Previous studies have shown that the metabolic switch that occurs in the compensatory stage of heart failure reflects a switch from the adult to fetal metabolic energy usage, which favours glycolysis (Turer *et al*., 2010; Lionetti *et al*., 2011). If heart disease is prolonged, cardiac hypertrophy progresses from a metabolically adaptive state to an uncompensated heart failure state. In end stage heart failure, energy metabolism is severely compromised as fatty acid oxidation is depressed and this results in an increase in circulating free fatty acids which ultimately inhibit the uptake and oxidation of glucose (Opie, 2004; Opie & Knuuti, 2009, Lionetti *et al*., 2011). The increase in circulating fatty acids is said to be associated with proteins which uncouple mitochondrial respiration thus affecting the efficiency of cardiac contraction in the already failing heart (Opie, 2004). The increased circulation of free fatty acids inhibit the uptake and oxidation of glucose thus if pronlonged

can result in hyperglycemia (Opie, 2004; Opie & Knuuti, 2009). It is known that in heart failure, energy metabolism is severely compromised and with the accumulation of free fatty acids this would constitute to metabolic dysregulation which can result in insulin resistance as well as abnormalities occurring in mitochondrial function which increase reactive oxygen species (ROS) (Opie & Knuuti, 2009).

1.4.1 AMP-activated Protein Kinase Regulation in Cardiac Metabolism

Central to the substrate switching is activation of adenosine 5'-monophosphate protein kinase (AMPK) (Allard *et al*., 1994 & Kahn *et al*., 2005). AMPK is often referred to as a metabolic fuel gauge and is involved in cellular glucose metabolism (Hardie & Carling, 1997; Viollet *et al*., 2007). When the heart is exposed to mechanical or metabolic stressors that increase cellular energy demand, AMPK is activated (Hardie & Carling, 1997; Dyck & Lopaschuk, 2006; Kola *et al*., 2006; Arad *et al* 2007; Viollet *et al*., 2007; Hock & Kralli, 2009). AMPK is activated by pathological stress such as glucose deprivation, oxidative stress and hypoxia (Kahn *et al*., 2005). In cardiac hypertrophy, a reduction in ATP and a rise in adenosine monophosphate protein (AMP) is detected thus activating AMPK which in turn inhibits ATP-consuming pathways and activates pathways which support ATP-production with less oxygen consumption (Hardie, 2003; Chan *et al*., 2004, Kahn *et al*., 2005, Allard *et al*., 2007; Zarrinpashneh *et al*., 2008). When metabolic demand is increased, the activation of AMPK plays an important role in gauging cardiac energy and in doing so increases glucose and fatty acid metabolism accordingly (Dyck & Lopaschuk, 2006). Studies have shown that the AMPKα_2 isoform is involved in metabolic responses of the heart to ischemia and is therefore

cardioprotective (Zarrinpashneh *et al*., 2006; Li *et al*., 2007). Although cardiac hypertrophy is employed to maintain metabolic demand through the activation of AMPK, prolonged functional load imposes metabolic stress therefore predisposing the heart to a further increase in functional and structural remodeling which is ultimately detrimental (Badeer, 1964; Chan *et al*., 2004). Previous investigators have attributed such deleterious effects to various cellular metabolic changes. These characteristics are said to be proportional to the progression of hypertrophy.

Here, excessive generation of ROS and subsequent pro-apoptotic events may ultimately compromise both mitochondrial and cardiac structural and functional integrity and lead to the progression of heart failure (Schreiber *et al*., 1973; Sawyer & Colucci, 2000; Tsutsui, 2006). Excessive accumulation of ROS in the mitochondria is deleterious to the function of the biological tissue (Ide *et al*., 1999; Tsutsui et *al*., 2006). The effects of ROS will be discussed in more detail in a later section of the introduction.

1.4.2 Transcriptional Regulation of Mitochondrial Biogenesis in Cardiac Hypertrophy

Mitochondrial biogenesis is a process that results in the growth and division of pre-existing mitochondria organelles and is controlled by the nuclear cell or mitochondrial DNA genome (Ventura-Clapier *et al*., 2008; Iglewski *et al*., 2010). Biogenesis of the mitochondria is triggered via environmental stresses such as exercise, oxidative stress, cell division and renewal and differentiation (Ventural-Clapier *et al*., 2008). Several transcription factors and other metabolic genes have been implicated in the development of mitochondrial biogenesis (Figure 1.1).

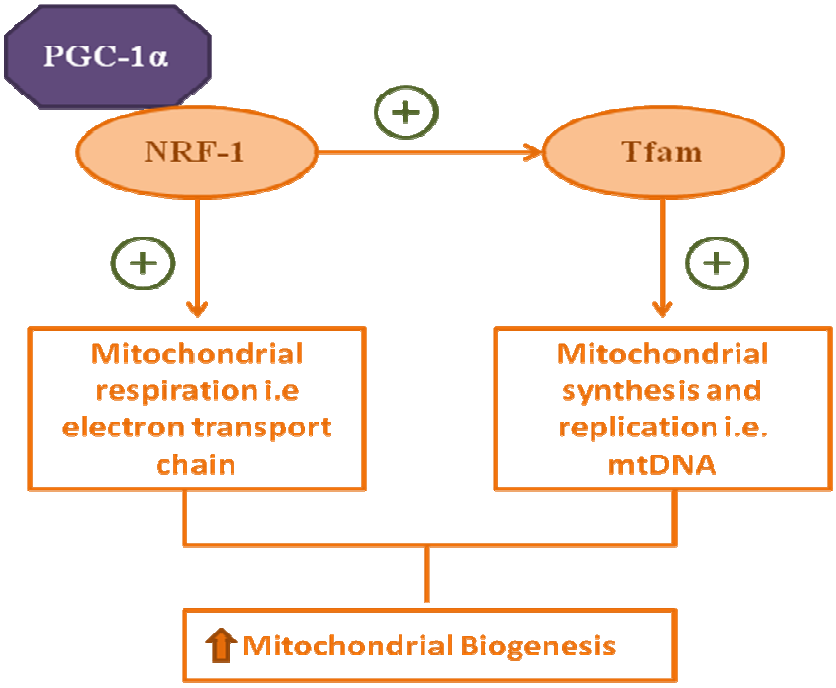

Figure 1.1 Schematic diagram representing the pathway which leads to the activation of mitochondrial biogenesis. '+' = activation; PGC-1α = peroxisome proliferator-activated receptor gamma co-activator 1α; NRF-1 = nuclear respiratory factor 1; Tfam = mitochondrial transcription factor A.

The activation of mitochondrial biogenesis cascade is induced by the activation of peroxisome proliferator-activated receptor gamma co-activator 1α (PGC-1α), which then increases the cardiac mitochondrial oxidative capacity by inducing nuclear respiratory factors 1 (NRF-1) and 2 (NRF-2) (Russell *et al*., 2005; Huss & Kelly 2005; Ventura-Clapier *et al*., 2008). PGC-1α co-activates the nuclear transcription factors as well as nuclear-encoded mitochondrial transcription factor A (Tfam) which is responsible for transcription and replication of mitochondrial DNA (Ventura-Clapier *et al*., 2008). Therefore cardiac specific deletion of Tfam will result in decreased levels of mitochondrial DNA, cardiac hypertrophy and ultimately progressive heart failure (Ventura-Clapier *et al*., 2008). The expression of Tfam is coordinated by NRF-1 and NRF-2 (Rimbaud *et al*., 2009).

These factors allow for transcriptional co-ordination between mitochondrial and nuclear activation during mitochondrial biogenesis (Ventural-Clapier *et al*., 2008). Mitochondrial biogenesis is activated as a long term response; however, it is not always activated when the energy demands increase (Hock & Kralli, 2009). PGC-1α is considered to be the master synchroniser of mitochondrial biogenesis and once activated increases the transcriptional activity of the nuclear respiratory factors which in turn promote the activity of mitochondrial transcription factor A, which then acts on the electron transport chain complex (Rosca & Hoppel, 2010). Studies have shown that activation of AMPK, under conditions of exercise, leads to the activation of PGC-1α thus co-activating mitochondrial respiration through the activation of NRF-1 as well as the activation of Tfam to promote an increase in mitochondrial number (Kelly & Scarpulla, 2004; Nishio *et al*., 2004; Kim *et al*., 2008). Not only does the activation of PGC-1α induce the activation of NRF-1 and Tfam but it also co-activates fatty

acid and glucose transport into the cell (Patten & Arany, 2011). The energy signal, AMPK, has been shown to prevent left ventricular hypertrophy by increasing bioenergetic capacity of the heart via upregulation of PGC-1α and NRF-1 (Rimbaud *et al*., 2009). Bergeron and colleagues (2001) investigated the effect of chronic energy stress on the activation of AMPK and whether this would lead to the activation of NRF-1 and ultimately activate the mitochondrial biogenesis pathway. After nine weeks of energy stress through a β-guanadinopropionic acid diet, AMPK played a role in skeletal muscle adaptation via the regulation of mitochondrial biogenesis and the expression of respiratory proteins through the activation of NRF-1 (Bergeron *et al*., 2001). Whether such metabolic changes may avert cardiac metabolic stress and its deleterious effects via activation of AMPK is currently not fully understood.

Using transmission electron microscopy to assist in identifying the mitochondria ultrastructure architecture, the modifications that can be seen in hypertrophy or heart failure are usually associated with decreases in mitochondrial number (Rosca & Hoppel, 2010).

1.5 Cardiac Energy Metabolism in Heart Failure

The role of the mitochondria in the heart is to ensure that it can perform optimally to meet the energy requirements of the body. The tissue within the heart muscle is highly oxidative and more than 90% of the energy supplied is derived from mitochondrial respiration (Ventura-Clapier *et al*., 2003). In cardiac hypertrophy, energy metabolism switches from fatty acid oxidation to glycolysis. Table 1.1 shows metabolic changes that have been observed as

pathological defects in the various animal models. The findings from studies which have investigated pressure overload induced hypertrophy are very similar to the cardiac structural and functional changes seen in the adrenergic model (see Table 1.1). However, with prolonged cardiac stress, glycolysis continues and the remodeling process leads to uncompensated energy metabolism which ultimately leads to loss of metabolic flexibility thus resulting in overall damage to the efficiency of the heart (Taegtmeyer *et al*., 2004).

A study investigating heart failure in the pressure overload model reported a close association of this model with deleterious LV remodeling (Norton *et al*., 2002). Another study investigating the changes in AMPK and metabolic adaptation to pressure overload reported that AMPK is involved in the switch from fatty acids to glucose in cardiac hypertrophy (Allard *et al*., 2007). The pressure overload model induces a change in the cellular energy state which activates AMPK when ATP levels decrease and this drives glycolysis in hypertrophy (Allard *et al*., 2007). Functional defects such as decreased cardiac contractility and contraction as well as resistance to fatigue are characteristic alterations of energy, in both skeletal and cardiac muscle (Garnier *et al*., 2003).

In conditions leading to cardiac hypertrophy, increases in plasma levels of catecholamines have been observed and this is said to be associated with various gene expression changes (Taimor *et al*. 2001). A study by Robinson and colleagues (2010) investigated the effect of β-adrenergic stimulation on mitochondrial biogenesis and found that there was no increase in mRNA for PGC-1α, Tfam and NRF-1 when skeletal muscle was assessed. However, whether the same alteration occurs in the failing myocardium is unknown.

1.6 The Formation of Reactive Oxygen Species in Heart Failure.

In the failing heart, reactive oxygen species (ROS) induce functional and structural damage of the myocardium and thus play an important role in the pathophysiology (Hill & Signal, 1996; Ide *et al*., 1999; Sawyer & Colucci, 2000; Ide *et al*., 2001; Tsutsui *et al*., 2008). Not only are the mitochondria the major site for the production of ROS but they are also susceptible to ROS-mediated deleterious effects that damage proteins, lipids and DNA (Ide *et al*., 2001, Murray *et al*., 2007 & Iglewski *et al*., 2010). The exact site of ROS production in the mitochondria occurs mainly at complex I and complex III in the electron transport chain (Ide *et al*., 1999; Kim *et al*., 2008). One of the causes of functional decline in the failing myocardium is prolonged oxidative stress which is as a result of mitochondrial DNA damage, further ROS generation and cellular injury (Murray *et al*., 2007).

Reductions in the mitochondrial DNA copy number bring about a decrease in mitochondrial RNA and protein thus leading to mitochondrial dysfunction (Ide *et al*., 2001). The outcomes of a study done by Ide and colleagues (2001) suggest that chronic increases in ROS production bring about mitochondrial damage and dysfunction thus leading to changes within cellular events thus resulting in myocardial remodeling and failure. Depression of mitochondrial respiratory capacity and whole heart oxidative capacity is characteristic of the failing heart (Bugger *et al*., 2010). Therefore, mitochondrial derangement that occurs in the failing heart could be attributed to ROS formation thereby inducing changes in the ultrastructure.

In heart failure, the activation of plasma renin activity and angiotensin-converting enzyme (ACE) contributes to the formation of angiotensin II which leads to an increase in oxidative

stress (Tsutsui *et al*., 2006). In heart failure the mitochondrial DNA are damaged and therefore myocardial remodeling results (Tsutsui *et al*., 2006). A study investigating pressure overload induced heart failure via pacing in dogs reported the presence of ROS and a decrease in complex I activity in the electron transport chain (Ide *et al*., 1999).

The acute effects of the β-adrenergic agonist, isoproterenol, on mitochondrial ROS production in mitochondrial cardiomyocytes reported that an increase in Ca^{2+}-independent signaling and ROS production is associated with contractile adaptive responses in this model (Andersson *et al*., 2011). The hyper-adrenergic effect of isoproterenol administration in conjunction with the activation of β-adrenergic receptors in heart failure leads to cardiac tissue damage and dysfunction as a result of prolonged increase in the production of ROS (Andersson *et al*., 2011). Administration of isoproterenol for seven days induces gene and protein expression of vascular proinflammatory cytokines IL-1β and IL-6 as well as altered vascular reactivity and oxidative stress (Davel *et al*., 2008). Not only does isoproterenol administration activate SNS and induce LVH, dysregulation of myocardial growth, dilatation and pump dysfunction, apoptosis, necrosis and reduced collagen linking through chronic adrenergic stimulation (Teerlink *et al*., 1994; Grimm *et al*., 1998; Taimor *et al*., 2001; Osadchii *et al*., 2006; Osadchii *et al*., 2007; Booysen *et al*., 2012) but inflammatory cytokines are also activated in the isoproterenol model (Davel *et al*., 2008).

1.7 The Effect of Metformin on Heart Failure.

Metformin is an orally administered drug that is commonly prescribed to patients with type 2 diabetes mellitus (Gundewar *et al*., 2009). Metformin lowers blood glucose (Gundewar *et al*., 2009) and has been proven to reduce insulin resistance (Cha *et al*., 2010; Cittadini *et al*., 2011). The presence of insulin resistance is a common characteristic in the development of chronic heart failure (Cittadini *et al*., 2011; Tuunanen & Knuuti, 2011). Table 1.3 is a summary of the studies which have looked at the effects of metformin administration on various models of hypertrophy and heart failure.

Studies have shown that metformin is a suitable choice of therapy to improve cardiac function in certain models of heart failure. The administration of metformin in conjunction with pressure-overload, adrenergic and doxorubicin-induced cardiotoxic animal models all showed beneficial cardioprotective properties (Gundewar *et al*., 2009; Cha *et al*., 2010; Yin *et al*., 2011; Wang *et al*., 2011; Cittadini *et al*., 2012 & Ashour *et al*., 2012). In contrast metformin administration in conjunction with volume-overload induced heart failure showed no beneficial effects (Benes *et al*., 2011). However, further investigation is necessary to determine how metformin exerts cardioprotective properties in chronic adrenergic-induced dilatation and pump dysfunction.

Table 1.3 Summary of studies involving animal models of heart failure and the effect of metformin administration.

Reference	Species/ Strain	Model	Metformin Dose & route	Study Duration	Effect of metformin
Cha *et al*., 2010	Mice	Adrenergic	150mg/kg/day	1 week	Partially inhibits hypertrophy, no activation of AMPK phosphorylation
Ashour *et al*., 2012	Wistar rats	Doxorubicin-induced cardiotoxicity	500mg/kg/day, p.o	11 days	Increased ATP levels, reduced reactive oxygen species, cardiomyocyte ultrastructure appeared almost normal, prevented cardiac hypertrophy
Gundewar *et al*., 2009	Mice	Pressure overload	125µg/kg/day, daily i.p	4 weeks	Improves LV structure and function and reduces LVH, improves mitochondrial respiration and ATP synthesis, promotes phosphorylation of AMPK and increases expression of PGC-1α.
Wang *et al*., 2011	Wistar rats	Pressure overload	100mg/kg/day, intragastric gavage	4 weeks	Reduced LVEDD and LVESD, increased AMPK, attenuated fibrosis and improved insulin resistance
Yin *et al*., 2011	SD rats	Pressure overload	250mg/kg/day, oral	12 weeks	Reduced myocardial infarct size, improved LV geometry, improved glucose and cellular energy metabolism
Benes *et al*., 2011	Wistar rats	Volume overload	300mg/kg/day, oral	21 weeks	No effect on AMPK activation, ATP content, mitochondrial function or arrangement. No improvement in cardiac performance
Cittadini *et al*., 2012	SHHF	Pressure overload	100mg/kg/day, oral	12 months	Reduced LV remodeling, reduced myocardial lipid accumulation. Restored myocardial contraction

Abbreviations: AMPK = adenosine 5' monophosphate protein kinase; PGC-1α = peroxisome proliferator-activated receptor gamma co-activator 1α; LVH = left ventricular hypertrophy; SD = Sprague Dawley rats; SHR = spontaneously hypertensive rats; WKY = Wistar Kyoto rats

The administration of metformin is known to indirectly activate AMPK thus increasing myocardial glucose uptake and reduce insulin resistance (Zhou *et al*., 2001; Opie & Knuuti, 2009; Cha *et al*., 2010; Cittadini *et al*., 2011). A study investigating the long term effects of AMPK activation reported that chronic activation of AMPK via the administration of metformin attenuates hypertrophic growth through the inhibition of protein synthesis and signaling pathways. Therefore metformin can be used to successfully target AMPK activation and thus inhibit cardiac hypertrophy and heart failure (Li *et al*., 2007). In a study by Gundewar and colleagues (2009), the administration of metformin for 4 weeks promoted an increase in AMPKα_2 and PGC-1α in cardiac hypertrophy thus improving mitochondrial respiration and preventing mitochondrial dysfunction and displaying cardioprotection. An increase in PGC-1α activity can inhibit the production of ROS, which are the trapped byproducts of mitochondrial respiration, by inducing uncoupling proteins thus reducing the mitochondrial membrane potential (Patten & Arany, 2011).

Cittadini and colleagues (2011) demonstrated that metformin reduces left ventricular dilation and wall stress thereby slowing down the development of left ventricular remodeling. Their results also showed that not only did metformin improve the systolic and diastolic cardiac function but the myocardial efficiency was restored to normal. Another study which investigated the administration of metformin in non-diabetic rats, with post-myocardial infarct pressure overload, identified protective effects of metformin on cardiac remodeling (Yin *et al*., 2011).

The results of both these studies prove to be important for clinical implications regarding the use of metformin as a cardioprotective drug. In contrast, long-term administration of

metformin to Wistar rats with aortocaval fistula volume-overload-induced hypertrophy showed no change in myocardial gene expression profile thus indicating that the presence of fatty acid oxidation is not dependent on genomic mechanisms and in this model metformin has no effect (Benes *et al*., 2011). According to Melenovsky and colleagues (2011), drug therapies administered to improve cardiac metabolism by improving insulin resistance might not be effective in the aorto-caval fistula model due to the hypoinsulinaemia present.

A study investigating isoproterenol-induced cardiac hypertrophy reported partial inhibition of metformin and a decrease in oxidative stress (Cha *et al*., 2010). Again in the volume overload model, chronic administration of metformin had no effect on the activation of myocardial AMPK, ATP content, mitochondrial function or morphology and overall metformin administration did not improve cardiac performance (Benes *et al*., 2011). Therefore, the exact effects of metformin seem to be determined by the type of animal model present and whether model-specific mechanisms promote the efficiency of metformin is still unknown. To date, the exact mechanisms through which metformin may counteract neurohormonal changes which induce heart failure are unknown. Furthermore, whether metformin exerts its cardioprotective effects via the activation of AMPK in neurohormonal models is unknown.

1.7 Study Objectives

Therefore the main questions that need to be investigated are the following: 1) Does metformin exert cardioprotective effects via the activation of AMPK in the neurohormonal

model of heart failure? 2) Are these beneficial effects medicated by changes in mitochondrial transcript gene expression and mitochondrial ultrastructure in the failing myocardium?

In order to address these questions, I will use a novel animal model of heart failure to identify a therapeutic strategy that could possibly protect the heart against functional and metabolic changes through the alteration of mitochondrial transcript gene expression and mitochondrial ultrastructure arrangement in this model. In doing so, isoproterenol will be administered for seven months to induce chronic adrenergic-induced cardiac dilatation and pump dysfunction. Our laboratory has repeatedly shown that chronic administration of isoproterenol induces cardiac dilatation and pump dysfunction (Osadchii *et al*., 2007; Booysen *et al*., 2012). In conjunction with this model, metformin will be administered chronically as a therapeutic strategy to assess whether mitochondrial transcript gene expression and mitochondrial ultrasctructure arrangement will be inhibited and therefore promote the restoration of cardiac function in the isoproterenol model of cardiac dilatation and pump dysfunction (Figure 1.2).

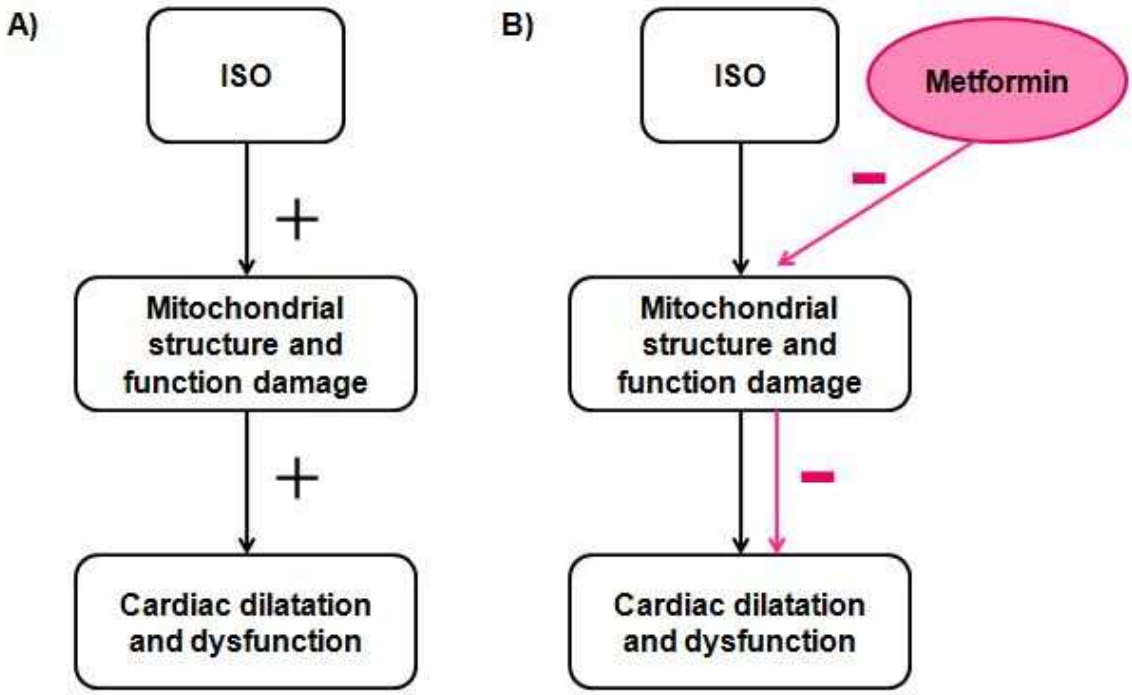

Figure 1.2 Schematic representation of hypothesis a) The effect of isoproterenol which results in cardiac dilatation and dysfunction. '+' = activate. b) The effect of co-administration of metformin on cardiac dilatation and dysfunction. '-' = inhibit.

Chapter 2

Materials and Methods

2.1 Materials

The following materials and reagents were used, with the supplier indicated in brackets: Transcriptor First Strand cDNA Synthesis kit (Roche Diagnostics GmbH, Penzberg, Germany), Accutrend® GCT Plus Meter (Roche Diagnostics GmbH, Mannheim, Germany), Accutrend® Triglyceride Test strips (Roche Diagnostics GmbH, Mannheim, Germany), LightCycler® FastStart DNA MasterPLUS SYBR Green kit (Roche Diagnostics GmbH, Mannheim, Germany), Aquasonic 100 Ultrasound Transmission Gel (Parker Laboratories, New Jersey, USA), Ascensia ELITE Blood Glucose Test Strips (Bayer Corp., Indiana, USA), Ascensia ELITE Glucose meter (Bayer Corp., Indiana, USA), ketamine (Bayer Pharmaceutical, Johannesburg, RSA), xylazine (Bayer Pharmaceutical, Johannesburg, RSA), GAPDH primers (Inqaba Biotechnical Industries, Pretoria, RSA), NRF-1 primers (Inqaba Biotechnical Industries, Pretoria, RSA), PGC-1α primers (Inqaba Biotechnical Industries, Pretoria, RSA), Tfam primers (Roche Diagnostics, Randburg, RSA), Isoproterenol hydrochloride (Sigma-Aldrich, Missouri, USA), metformin (Sigma-Aldrich, Missouri, USA), liquid nitrogen (Afrox, Germiston, RSA), NucleoSpin® RNA II kit (MACHEREY-NAGEL, Germany), QIAShredder kit (QIAGEN, Hilden, Germany), RNA Later® solution (Applied Biosystems/Ambion, California, USA), RNaseZap® wipes (Ambion Inc., Texas, USA), Sabax sodium chloride 0.9% saline (Adock Ingram, Midrand, RSA).

2.2 Methods

2.2.1 Ethics Approval

All procedures were approved by the Animal Ethics Screening Committee of the University of the Witwatersrand (Ethics Clearance Number: 2010/27/04) (See Appendix B).

2.2.2 Animal Model and Drug Administration

A total of 48 male Sprague-Dawley rats weighing 290-350g were obtained from the Central Animal Service (CAS) unit of the University of the Witwatersrand. The animals were housed individually in cages and kept at the CAS unit in a temperature controlled room with a 06:00 - 18:00 light regime. The rats were allowed access to rat chow and water *ad libitum*. A total of eight fatalities were recorded in the duration of the study, as in some cases isoproterenol induced cardiac arrest after injection. Fatalities occurred in the isoproterenol group and the isoproterenol+metformin group. The final analysis for this study was completed using the remaining forty rats.

Initially, the forty-eight male rats were randomly assigned to four groups, each with a sample size of 12. The groups were as follows: vehicle control (CONT), metformin (MET), isoproterenol (ISO) and isoproterenol and metformin (ISO+MET). The CONT group received a daily subcutaneous injection of $0.1ml.kg^{-1}.day^{-1}$ of 0.9% saline. The MET group received $300mg.kg^{-1}.day^{-1}$ of metformin, dissolved in drinking water and administered orally, and a daily subcutaneous injection of $0.1ml.kg^{-1}.day^{-1}$ of 0.9% saline. The ISO group received a

daily subcutaneous injection of isoproterenol at a dose of 0.02mg.kg^{-1}.day^{-1} and the ISO+MET group received both isoproterenol and metformin as per the above mentioned doses and route as shown in Fig 2.1.

Saline injections were administered 5 days prior to the initial isoproterenol injections. This was done to habituate the rats to animal handling and drug administration. The initial isoproterenol dose was set at 0.01mg.kg^{-1}.day^{-1} for a week to prevent early cardiac arrest: thereafter the dosage was raised to 0.02mg.kg^{-1}.day^{-1} for seven months. The 0.02mg.kg^{-1}.day^{-1} dose of isoproterenol has previously been used in our laboratory to elicit the development of heart failure upon chronic isoproterenol administration (Woodiwiss *et al*., 2001 and Osadchii *et al*., 2006). The 300mg.kg^{-1}.day^{-1} dose of metformin had been previously established in our laboratory to investigate cardioprotective properties when co-administered with the isoproterenol model (unpublished data). Water bottles were weighed to ensure that the individually-caged animals were taking up appropriate amounts of metformin. All treatments were administered daily for seven months.

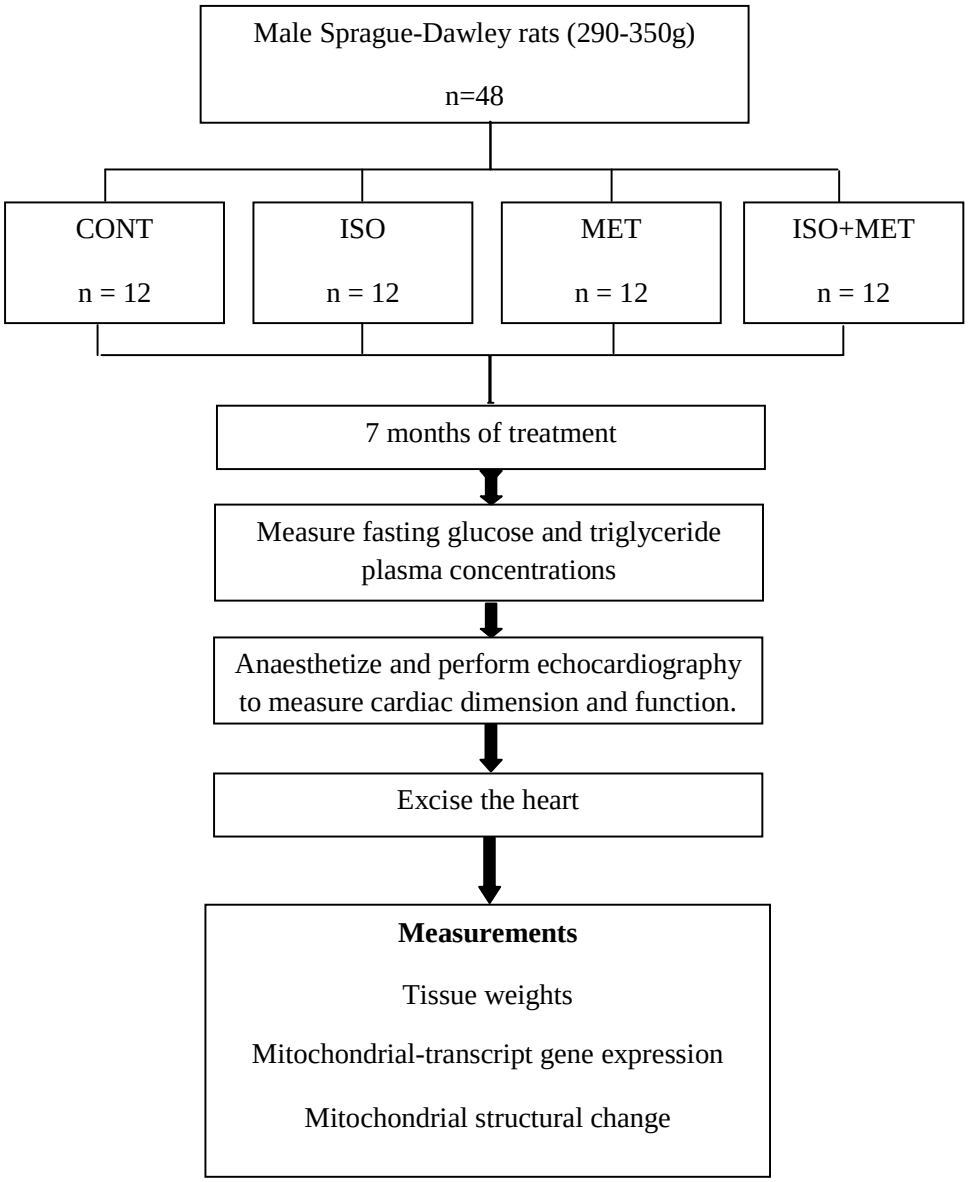

Figure 2.1 Experimental Design indicating the number of male Sprague-Dawley rats used and the duration of treatment prior to the termination and the measurements obtained. CONT = control, ISO = isoproterenol, MET = metformin and ISO+MET = isoproterenol and metformin.

2.2.3 Measurement of Body Mass

All animals were weighed once weekly to monitor body mass changes. An average monthly body mass value, for each of the groups, was recorded and plotted on a graph to assess the trends in the body mass following seven months of treatment. The initial body mass and the final body mass values were used to calculate the percentage body mass gain using the formula below:

$$\% \text{ body mass gain} = \frac{(\text{final body mass} - \text{initial body mass})}{\text{Initial body mass}} \times 100$$

2.2.4 Measurement of Glucose and Triglyceride Plasma Concentrations

After seven months of treatment, the animals were fasted overnight for 16 hours. The animals were placed in constrainers and a sterile needle was used to perforate the tail vein. A drop of blood was collected on an Ascensia ELITE blood-glucose test strip, which was then placed in an Ascensia ELITE glucose meter to determine fasting blood glucose plasma concentration. To determine triglyceride plasma concentration, a drop of blood was collected on a triglyceride test strip and placed in Accutrend Glucose-Cholesterol-Triglyceride Plus meter.

2.2.5 Echocardiography

Immediately after the determination of fasting glucose and triglyceride plasma concentrations, the rats were anaesthetised using an intraperitoneal injection of ketamine ($75 mg.kg^{-1}$) and

xylazine (15mg.kg^{-1}). Once the rats were under anaesthesia they were weighed to record final body mass. To determine left ventricular chamber function and left ventricular dimensions *in vivo*, two-dimensional targeted M-mode echocardiography was performed using a 7.0MHz transducer and an ACUSON CYPRESS portable echocardiograph machine (Siemens Medical Division, USA), as previously described (Woodiwiss *et al*., 2001, Norton *et al*., 2002). Briefly, after shaving the rat's chest, the rat was placed in the prone position in a holding container with the chest visible through an open window on the base of the container. The high-resolution ultrasonic probe together with Aquasonic ultrasound gel was inserted through the open window at the base of the container and placed on the rat chest wall to obtain echocardiographic images.

A two dimensional image of the short axis of the left ventricle at the level of the papillary muscle was obtained. The image was considered to be of high quality if the endocardial surface of both the anterior wall and the posterior wall were clearly visible throughout systole and diastole (Figure 2.2). Cardiac dimensions were recorded in centimetres and three or more measurements were obtained for each left ventricular dimension. Left ventricular internal dimensions and posterior wall thickness were measured at the end of systole and at the end of diastole according to the American Society for Echocardiography's leading edge method (Sahn *et al*., 1978) (Figure 2.2). Left ventricular endocardial fractional shortening (FS_{end}) and midwall fractional shortening (FS_{mid}) were the indices used to determine chamber and myocardial function, respectively (Norton *et al*., 2002). The equations below were used to calculate the FS_{end} and FS_{mid}.

$$FS_{end} = \frac{LVEDD - LVESD}{LVEDD} \times 100$$

Where

LVEDD = Left ventricular end diastolic internal diameter

LVESD = Left ventricular end systolic internal diameter

$$FS_{mid} = \frac{(LVEDD + LVED\ PWT) - (LVESD + LVES\ PWT)}{(LVEDD + LVED\ PWT)} \times 100$$

Where

LVED PWT = Left ventricular end diastolic posterior wall thickness

LVES PWT = Left ventricular end systolic posterior wall thickness

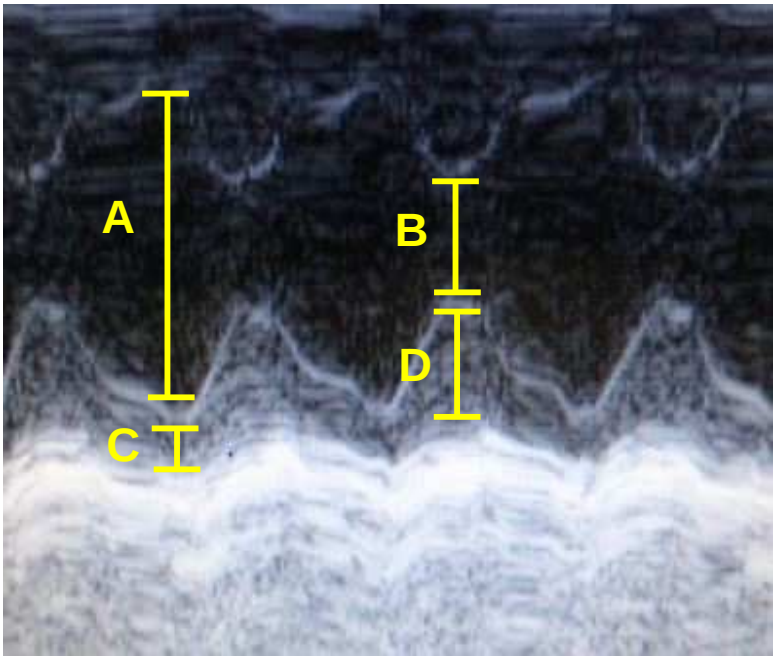

Figure 2.2 Sample recording illustrating left ventricular dimensions using two-dimensional targeted M-mode echocardiography. A = LV end diastolic internal diameter (LVEDD), B = LV end systolic diameter (LVESD), C = LV end diastolic internal diameter posterior wall thickness (LVEDD PWT), D = LV end systolic posterior internal diameter wall thickness (LVESD PWT).

2.2.6 Collection of Tissue Samples

Immediately after echocardiography, the rats were administered more anaesthetic and the hearts were harvested from the animals and weighed. The left and right ventricles were separated and weighed. The left ventricular tissue was either used immediately or stored for subsequent analysis. For gene expression analysis the left ventricular tissue was stored in RNA Later® solution at -20°C. For every 1.8g of left ventricular tissue, 1.8ml of RNA Later® solution was used. For mitochondrial analysis, a small rectangular longitudinal section was cut from the left ventricular tissue and stored in 2.5% glutaraldehyde and 2% paraformaldehyde in 1 X phosphate buffered saline (137mM NaCl, 2.7mM KCl, 10mM Na_2HPO_4, 1.8mM KH_2PO_4) (pH 7.3) (see Appendix A) for Transmission Electron Microscopy analysis. Tibia from the left leg was de-fleshed, using a scalpel, and the length measured with a string and ruler. Tibial length was determined to assess bone growth of the rats. According to Yin and colleagues (1982), the measurement of tibial length reflects a better reference of body size as it can represent relative lean body size throughout the life of the rat and it is said to be physiologically linked to the metabolic demands exerted on the heart by the body.

2.2.7 Measurement of Gene Expression

2.2.7.1 Total mRNA isolation

All work surfaces were kept sterile by using RNaseZap® wipes and UV light disinfection, thereby reducing contamination. The stored left ventricular tissue in RNA Later solution was

thawed and placed on ice. From each sample tube, 300µl of RNA Later solution was aliquoted into fresh microcentrifuge tubes to ensure the tissue did not dry out. Using a balance, 50mg of left ventricular tissue from each animal specimen was weighed and placed in a labeled microcentrifuge tube with the 300µl RNA Later solution. Using sterile forceps, the 50mg of left ventricular tissue was then transferred into an autoclaved porcelain mortar and liquid nitrogen was used to flash-freeze the ventricular tissue. A sterile porcelain pestle was then used to homogenise the ventricular tissue. The homogenised tissue or rather powder was transferred into a labeled microcentrifuge tube. Total mRNA isolation was performed using a NucleoSpin® RNA II kit. All reagents/buffers in the kit were reconstituted according to the manufacturer's instructions. For tissue lysis, 345µl of RA1 buffer was added to the labeled microcentrifuge tubes containing the homogenised left ventricular tissue. The tubes were vortexed at maximum setting for five minutes. The contents of each tube were then pipetted into QIAShredder™ column disruptors which were used to further homogenise the tissue lysate in order to reduce viscosity. The QIAShredder™ column disruptors were centrifuged for five minutes at 20^{o}C (11,218 x g) and the supernatant added to NucleoSpin® Filter columns to further remove insoluble debris from the lysate. The filter columns were centrifuged for five minutes at 20°C (11,218 x g). To ensure RNA binding, 350µl 70% ethanol was added to the supernatant and mixed by reverse pipetting. The supernatant of each sample was added into NucleoSpin® RNA II filter columns. The filter columns were centrifuged for one minute at 20°C (11,218 x g). The supernatant was then discarded and the filter columns were transferred into 2ml collection tubes. The membrane was dried by adding 350µl of membrane desalting buffer to the filter columns and centrifuged for one minute at

20°C (11,218 x g). By removing the salt from the membrane, the rDNase was able to be absorbed more effectively. To digest DNA, a DNase reaction mixture was prepared in a sterile 1.5ml microfuge tube by mixing 10µl of reconstituted rDNase with 90µl reaction buffer for rDNase for each sample. From the reaction mixture, 95µl was added directly to the silica membrane in the filter column and incubated at 25°C for 15-30 minutes. The silica membrane of the filter column was washed and dried to inactivate the rDNase by adding 200µl RA2 buffer and centrifuging for one minute at 20°C (11,218 x g). Thereafter, 600µl RA3 buffer was added and centrifuged for two minutes at 20°C (11,218 x g). Lastly, 250µl RA3 buffer was added to the filter columns and centrifuged for two minutes at 20°C (11,218 x g). The filter columns were then placed into 1.5ml nuclease-free collection tubes and 60µl RNase-free water was added to elute the RNA. The tubes were centrifuged for one minute at 20°C (11,218 x g) and 10µl of the eluted RNA was aliquoted into microcentrifuge tubes and stored at -70°C for subsequent analysis.

2.2.7.2 Complementary DNA (cDNA) synthesis

Aliquoted mRNA samples were thawed and placed on ice. cDNA was synthesised using a 1st Strand cDNA Reverse Transcription kit according to the manufacturer's instruction. A master mix consisting of 2µl polymerase chain reaction (PCR)-grade water and 1µl anchored-oligo (dT) 18 primer was made up for each sample. The samples were then incubated in a ThermoHybaid Px2 PCR Thermocycler (Applied Biosystems, USA) at 65°C for ten minutes. Th4is temperature initiated the annealing and extension of the cDNA. Another master mix consisting of 4µl transcriptor reverse transcriptase (RT) reaction buffer, 0.5µl protector RNase

inhibitor, 2µl deoxynucleotide mix and 0.5µl transcriptor reverse transcriptase was made up for each sample. From this master mix, 7µl was added to each sample tube and inversely pipetted to mix the contents. The samples were then pulse centrifuged and incubated for 30 minutes at 55°C. At this temperature the DNA continued to anneal and extend. The temperature was then increased to 85°C for five minutes to denature and inactivate cDNA synthesis. The same pool of cDNA was used for both the target and control reactions. Once complete, the cDNA samples were stored at -20°C for subsequent analysis.

2.2.7.3 Quantitative Real-Time Polymerase Chain Reaction (RT-PCR)

The stored cDNA samples were thawed and placed on ice. A single primer set was used for each RT-PCR experimental run, which was performed on samples from the control and treatment groups. This was done due to the limited number of glass capillary slots on the RT-PCR loading carousel. The following forward and reverse primers were used: adenosine 5´ monophosphate-activated protein kinase alpha 2 ($AMPK\alpha_2$), peroxisome proliferator activated receptor gamma co-activator 1 alpha (PGC-1α), nuclear respiratory factor (NRF-1), mitochondrial transcription factor A (Tfam) and glyceralydehyde-3-phospate dehydrogenase (GAPDH) (Table 2.1). GAPDH was used as a housekeeping gene as it is ubiquitously expressed in the tissue. The transcriptional targets: PGC-1α, NRF-1, Tfam and AMPKα2 were amplified using a LightCycler 1.5 real time-PCR machine (Roche diagnostics, Mannheim, Germany) according to manufacturer's instructions. The correct reaction programs for the real time-PCR templates were optimised previously during my Honours degree (Peterson, unpublished) (see Table 2.2).

Table 2.1 Primers used for real-time PCR amplification

Gene	Sense	Sequence
AMPKα2	Forward	5´-CAGGGACTGCTACTCCACAGAGA-3´
	Reverse	3´-CCTTGAGCCTCAGCATCTGAA-5´
PGC-1α	Forward	5´-ATCACCCGAGAGTTCCTAAA-3´
	Reverse	3´-CCGATCTCCACAGCAAATTAT-5´
NRF-1	Forward	5´-CATTAGATGAATATACGACACGAGT-3´
	Reverse	3´-CTCCAGGTCTTCCAGGAT-5´
Tfam	Forward	5´-CATACCCTCGCCTGTCA-3´
	Reverse	3´-ATCAGTTCTGAAACTTTTGCAT-5´
GAPDH	Forward	5´-ATGCCATCACTGCCACCC-3´
	Reverse	3´-GCCTGCTTCACCACCTTCTT-5´

AMPKα2 = adenosine 5' monophosphate-activated protein kinase alpha 2; PGC-1α: peroxisome proliferator activated receptor gamma co-activator 1-alpha = NRF-1 = nuclear respiratory factor-1; Tfam = mitochondrial transcription factor A; GAPDH = glyceraldehyde-3-phosphate dehydrogenase.

Table 2.2 Optimised primer LightCycler® experimental cycling conditions

Template	Activation program	PCR program	Melt program	Cool program
AMPKα2	1 cycle: 95°C for 10 mins	35 cycles: 95°C for 5 sec 51°C for 15 sec 72°C for 10 sec	1 cycle: ramp temperature - 65°C for 30 sec (20°C/sec)	1 cycle: 40°C for 30 sec
GAPDH	1 cycle: 95°C for 10 mins	40 cycles: 95°C for 5 sec 56°C for 15 sec 72°C for 10 sec	1 cycle: ramp temperature - 65°C for 30 sec (20°C/sec)	1 cycle: 40°C for 30 sec
NRF-1, Tfam	1 cycle: 95°C for 10 mins	40 cycles: 95°C for 5 sec 52°C for 15 sec 72°C for 10 sec	1 cycle: ramp temperature - 65°C for 30 sec (20°C/sec)	1 cycle: 40°C for 30 sec
PGC-1	1 cycle: 95°C for 10 mins	40 cycles: 95°C for 5 sec 55°C for 15 sec 72°C for 10 sec	1 cycle: ramp temperature - 65°C for 30 sec (20°C/sec)	1 cycle: 40°C for 30 sec

AMPKα2 = adenosine 5' monophosphate-activated protein kinase alpha 2; PGC-1α = peroxisome proliferator activated receptor gamma co-activator 1-alpha; NRF-1 = nuclear respiratory factor-1; Tfam = mitochondrial transcription factor A; GAPDH = glyceraldehyde-3-phosphate dehydrogenase.

The melt programs specified in Table 2.2 are the approximate ramp rate temperatures as opposed to the actual melting point temperature which is a fixed temperature. All real-time PCR runs were performed in duplicate, and each reaction mixture was prepared using the LightCycler FastStart DNA Master^{PLUS} SYBR Green I kit (Roche) in a total volume of 20µl: 12µl PCR-grade water, 1µl of each primer, forward and revers (primer final concentration 100pmol/µl), 4µl Master mix and 2µl cDNA template.Figure 2.3 represents an example of a sigmoidal amplification curve obtained from GAPDH. The increase in fluorescence amplification indicates the presence of DNA. If the samples had no DNA there would be no curve. After each run a similar amplification curve will be generated. Because SYBR Green I dye is a non-specific fluorescent intercalating binding dye it binds to double-stranded DNA in a sequence-independent way. Therefore to ensure non-specific PCR products are rule out and only the specific products have been amplified, a melting curve analysis was performed after amplification (see Figure 2.4). Figure 2.4 is an example of the melting curve generated for GAPDH and shows a single melting curve which is representative of a single species of DNA molecule. Using, the LightCycler® Software version 4.1 (Roche Diagnostics, Mannheim, Germany), analysis of the target transcripts (PGC-1α, NRF-1, Tfam and AMPKα2) were relatively quantified. As the samples were run in duplicate, the target and housekeeping/reference genes were amplified from the same sample. Therefore, by determining the ratio between the amounts of target gene and housekeeping gene (GAPDH), for all the samples, gene expression levels could be calculated (as explained in the software user manual).

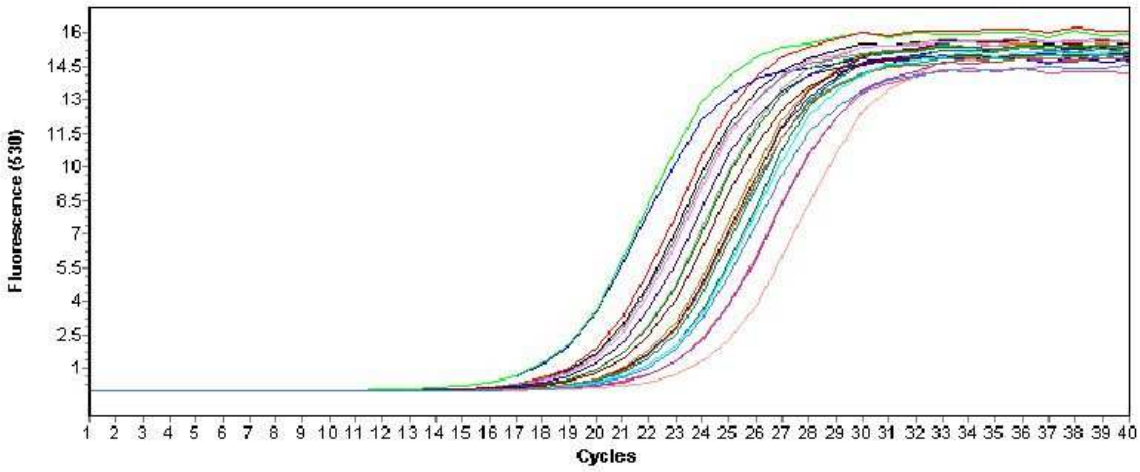

Figure 2.3 Amplification curve generated for GAPDH using real-time PCR. The plotted curve shows the increasing fluorescence for all the samples ran in duplicate for the target gene. GAPDH = glyceraldehyde-3-phospate dehydrogenase.

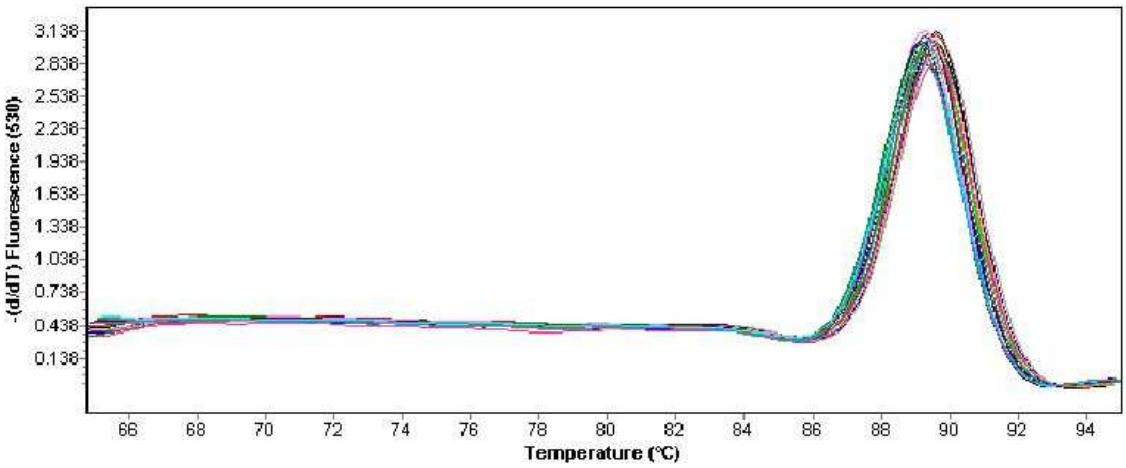

Figure 2.4 Melting curve generated for GAPDH using real-time PCR. Single peak confirms specific PCR product with a characteristic melting point of 89.5^{o}C. GAPDH = glyceraldehyde-3-phosphate hydrogenase.

2.2.8 Transmission Electron Microscopy

Transmission Electron Microscopy (TEM) was used to assess the mitochondrial and myofibrillar structural changes following treatment with isoproterenol and metformin. The 1µM gold ribbon sections and the electron micrographs studied were prepared in the Microscopy and Microanalysis Unit, School of Anatomical Sciences, Faculty of Health Sciences, University of the Witwatersrand, Johannesburg.

2.2.8.1 Left ventricular tissue fixation

Thin rectangular sections taken from the left ventricular tissue of the Sprague-Dawley hearts; were fixed in 2.5% gluteraldehyde and 2% paraformyldehyde in 1X PBS (pH 7.3) for 1 hour. The specimens were then cut into small 3 x 1 mm sections and left to fix for a further 2 hours. Thereafter, the specimens were rinsed with PBS (pH 7.3) twice for 30 minutes and were stored in the fridge at 4^{o}C. The PBS was then discarded and 398 µl 1% osmium tetroxide dissolved in PBS was pipetted into each specimen vial and left to stand for 1 hour to preserve the specimen. The osmium tetroxide was then discarded and the specimens were rinsed with PBS for 1 hour and were then stored in PBS overnight.

2.2.8.2 Dehydration and embedding of samples

Samples were dehydrated by sequentially immersing them, at 15 minute intervals, in increasing ethanol concentrations (50%, 70%, 80%, 95% and 100%). While dehydration with

80% ethanol took place, the resin mix (Araldite, Epon 812, DDSA) (see Appendix A for recipe) was made up and left to gently mix on a vertically rotating mixer.

After the dehydration process, the 100% ethanol was removed and enough 100% propylene oxide was added to completely immerse and infiltrate the samples, for 20 minutes. The 100% propylene oxide was discarded and more 100% propylene oxide was added for additional 20 minute incubation. Thereafter, the propylene oxide was discarded and 2ml 50% propylene oxide/50% resin was added to each sample and left for one hour. The 50% propylene oxide/50% resin was then discarded and resin mix (see recipe in Appendix A) was added and left overnight.

On the day of embedding, 0.7g DMP30 hardening accelerator was added to 26g of resin (see Appendix A) and mixed on the rotating mixer for one hour. Thereafter, the overnight resin was discarded and the samples were individually placed into a resin block mould. Using a syringe, the resin with hardening accelerator was added to each labeled specimen block to embed overnight at room temperature. This was done to ensure maximum infiltration of resin into the specimens. 24 hours later, the resin moulds were freed of air bubbles and baked in the oven at 60^{o}C for 48 hours. Once baking was completed, the resin blocks were removed from moulds and were ready for sectioning.

2.2.8.3 Sectioning of embedded resin blocks

Glass knives were made using a Knife Maker Type 7801A LKB (Stockholm, Bromma, Sweden). Candle wax and electrical tape were used to make up boats that were filled with

water and used to collect the 1µM gold ribbons. An Ultramicrotome Ultracut (Riechert-Jung, Austria) was used to cut sample-embedded resin blocks into ultrathin sections with a silver/gold interference colour these are referred to as 1µM gold ribbons. Xylene vapour was used to smooth out the ribbons before they were collected on the viewing grids.

2.2.8.4 Staining of grids

Beforehand, 0.05-0.1g of uranyl acetate was dissolved in 100% methanol. To obtain a 1% lead citrate solution, 0.25g lead citrate was dissolved in 25ml distilled water and 1ml 4% sodium hydroxide (NaOH). Both the uranyl acetate and lead citrate were centrifuged for 10 minutes at 3000 rpm. Three 50ml beakers containing 50% methanol were then prepared. Parafilm was used to cover a glass petri-dish and filter paper was readily available. After centrifugation, the uranyl acetate mixture was covered with foil due to light sensitivity. A few drops of the uranyl acetate mixture were placed on the parafilm-covered petri-dish. Another petri-dish was used to cover the drops and prevent inhalation of any uranyl acetate fumes. The number of drops was dependent on the number of grids. Grids were allowed to stain for three minutes. Thereafter each grid was rinsed in the three 50% ethanol beakers, by dipping each grid ten times in each beaker, and allowed to dry for 10 minutes on filter paper. New parafilm was placed on the glass petri-dish. Once the grids were dry, a few drops of 1% lead citrate were placed on the petri-dish and the grids were again stained for three minutes. Thereafter, the grids were rinsed by dipping each grid ten times in one beaker of 0.1M NaOH and ten times in three beakers of distilled water. The grids were left to dry on filter paper before being ready to view.

2.2.8.5 Viewing grids with TEM

The grids were viewed and four-to-six micrographs per sample were taken at 5000x magnification on 80keV using JEOL JEM-100S Transmission Electron Microscope (JEOL, Japan). These were used in quantification to assess mitochondrial structural changes. Using AutoCAD 2007 software, the total area occupied by the mitochondria was determined relative to the total area of the micrograph thus termed relative mitochondrial area.

2.3 Statistical Analysis

All statistical analysis was performed using GraphPad Prism version 5.0 for Windows (GraphPad Software, San Diego, California, USA). The values are expressed as mean ± SEM. A statistical comparison of variables between controls and treatment groups were performed using a one-way analysis of variance (ANOVA) with a Tukey *post hoc* test, comparing differences between all the groups. A p-value <0.05 were considered significant.

Chapter 3

Results

3.1 Chronic administration of isoproterenol and metformin reduced final body mass and the body mass gain.

Table 3.1 and Figure 3.1 shows the effect of chronic isoproterenol and metformin administration on final body mass, the percentage body mass gain, tibial length and heart mass. No statistical significance was seen in the initial body mass of the animals (Table 3.1). However, seven months of daily isoproterenol and metformin administration significantly decreased the final body mass in the ISO+MET group when compared to the CONT (CONT, 680.75±17.84 vs. ISO+MET, 601.88±18.13; p=0.0132) and the MET (MET, 689.75±19.00 vs. ISO+MET, 601.88±18.13; p=0.0132) groups (Table 3.1; Figure 3.1). Also, a significant reduction in the percentage body mass gain was observed within the ISO+MET group when compared to the CONT (CONT, 131.91±0.03 vs. ISO+MET, 105.07±6.27; p=0.0083) and the MET (MET, 136.05±6.45 vs. ISO+MET, 105.07±6.27; p=0.0083) groups (Table 3.1; Figure 3.1).

Following seven months of chronic isoproterenol and metformin administration, no statistical differences were seen in the tibial length, heart mass, left ventricular mass, heart mass-to-tibial length ratio (HM/TL) and the left ventricular mass-to-tibial length ratio (LVM/TL) (Table 3.1; Figure 3.1). However, when body mass was adjusted for tibial length, as an index of bone growth, there was a significant reduction in the ISO+MET group when compared to the CONT group (CONT, 141.80±3.46 vs. ISO+MET, 122.83±3.62; p=0.0044) (Table 3.1; Figure 3.1)

The chronic co-administrative drug effect of isoproterenol and metformin decreased the final body mass and the percentage body mass gain. Adjusting for tibial length is an index of growth as opposed to adjusting for body mass which is an index of body mass gain. Heart mass and left ventricular mass were adjusted to tibial length to assess the presence of cardiac hypertrophy. However, isoproterenol and metformin administration did not alter heart mass and left ventricular mass even when adjusted for tibial length thus there was no presence of cardiac hypertrophy. Although body mass-to-tibial length ratio was decreased in the ISO+MET group, the co-administrative effect of isoproterenol and metformin was as a result of a decrease in body mass and not due to the effect of bone growth thus the administration of isoproterenol and metformin reduced body mass.

Table 3.1 Chronic administration of isoproterenol and metformin decreased the body mass gain but did not alter the heart mass in rats.

	CONT (n=12)	**ISO (n=8)**	**MET (n=12)**	**ISO+MET (n=8)**
Body mass initial (g)	293.67±2.39	296.88±3.14	292.33±2.45	293.63±2.98
Body mass final (g)	680.75±17.84	644.88±19.93	689.75±19.00	601.88±18.13***$**
% Body mass gain	131.91±6.17	117.26±6.38	136.05±6.45	105.07±6.27*$
Tibial length (cm)	4.80±0.03	4.90±0.06	4.90±0.05	4.90±0.08
HM (g)	1.45±0.05	1.48±0.04	1.38±0.04	1.34±0.04
LVM (g)	1.10±0.03	1.15±0.04	1.08±0.03	1.05±0.03
BM/TL (g/cm)	141.80±3.46	131.61±3.79	140.76±3.88	122.83±3.62*$
HM/TL (g/cm)	30.21±0.93	30.23±0.84	28.16±0.81	27.34±0.76
LVM/TL (g/cm)	22.92±0.59	23.47±0.71	22.04±0.64	21.43±0.67

Measurements were obtained following seven months of isoproterenol and metformin administration. HM = heart mass, LVM = left ventricular mass, BM/TL = body mass final adjusted to tibial length. CONT = control group, ISO = isoproterenol group, MET = metformin group, ISO+MET = isoproterenol+metformin group. Values are represented as means±SEM and were analysed using one-way ANOVA with Tukey *post hoc* test. *$p<0.05$ versus CONT, $ $p<0.05$ versus MET.

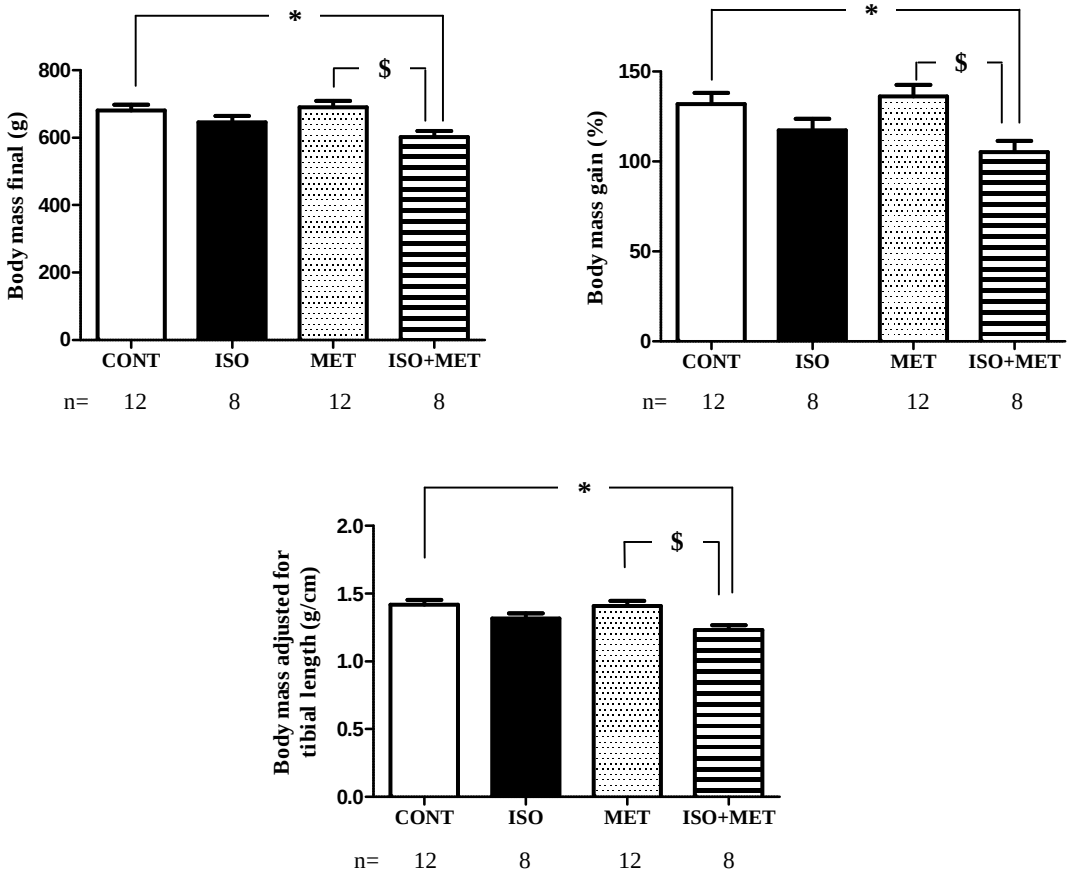

Figure 3.1 Chronic administration of isoproterenol and metformin decrease the body mass gain as a result of drug interaction. CONT = control, ISO = isoproterenol, MET = metformin, ISO+MET = isoproterenol+metformin.. Values are represented as means±SEM and were analysed using one-way ANOVA with Tukey *post hoc* test. *****$p < 0.05$ versus CONT, $^{\$}p < 0.05$ versus MET.

3.2 Chronic co-administration of metformin reduced fasting plasma glucose.

Prior to termination, the animals were fasted overnight for 16 hours and fasting plasma glucose and triglyceride levels were measured (Table 3.2). After seven months of daily administration with isoproterenol and metformin, there was a statistically significant decrease in fasting plasma glucose in the ISO+MET group when compared to the CONT group (CONT, 4.15±0.19 vs. ISO+MET, 3.45±0.21; p=0.0150), using the one-way ANOVA with a Tukey post hoc test (Table 3.2). However, on closer inspection using a one-way ANOVA with a Dunnett post hoc test to compare the intervention groups to the CONT group, a significant decrease was seen in both the MET (CONT, 4.15±0.19 vs. MET, 3.64±0.08; p=0.0150) and ISO+MET (CONT, 4.15±0.19 vs. ISO+MET, 3.45±0.21; p=0.0150) groups when compared to the CONT group. Seven months of chronic isoproterenol and metformin administration produced no statistical significance in triglyceride levels. The administration of metformin alone showed no effect on fasting plasma glucose. However, when metformin was administered in conjunction with isoproterenol, fasting plasma glucose was decreased and no changes were seen in triglyceride levels.

Table 3.2 Chronic administration of isoproterenol decreased fasting plasma glucose when co-administered with metformin

	CONT (n=12)	**ISO (n=8)**	**MET (n=12)**	**ISO+MET (n=8)**
Fasting blood glucose (mmol/l)	4.15±0.19	3.86±0.08	3.64±0.08	3.45±0.21*****
Triglycerides (mmol/l)	1.58±0.10	1.47±0.07	1.78±0.12	1.66±0.09

Measurements were taken after seven months of treatment. CONT = control, ISO = isoproterenol, MET = metformin, ISO+MET = isoproterenol+metformin. Values are represented as means±SEM and were analysed using one-way ANOVA with Tukey *post hoc* test. ***** $p<0.05$ versus CONT.

3.3 Metformin prevents isoproterenol-induced left ventricular dilatation and dysfunction.

Figure 3.3.1 shows the indices that were used to assess cardiac dimension and left ventricular myocardial function. Following seven months of treatment with isoproterenol and metformin, the ISO group showed a significant increase in LVEDD when compared the CONT (CONT, 7.92±0.19 vs. ISO, 8.76±0.21; p=0.0013), MET (MET, 7.55±0.15 vs. ISO, 8.76±0.21; p=0.0013) and ISO+MET (ISO+MET, 7.63±0.29 vs. ISO, 8.76±0.21; p=0.0013) groups. For the LVESD, there was a similar significant increase in the ISO group when compared to the CONT (CONT, 4.43±0.16 vs. ISO, 5.49±0.16; p<0.0001), MET (MET, 4.09±0.15 vs. ISO, 5.49±0.16; p<0.0001) and ISO+MET (ISO+MET, 4.04±0.25 vs. ISO, 5.49±0.16; p<0.0001) groups. There were no significant differences found in LVED PWT amongst all the groups. The ISO group showed significant reduction in LVES PWT when compared to the CONT group (CONT, 3.10±0.05 vs. ISO, 2.82±0.12; p=0.0174). Therefore, in the ISO group there was evidence of reduced LVEDD which resulted in compromised contractility and cardiac dilatation. However, co-administration of metformin prevents the left ventricular dilatation and dysfunction.

Using the above indices and established formulae I calculated the endocardial fractional shortening (FS_{end}) and the mid-wall fractional shortening (FS_{mid}) to assess left ventricular chamber function and myocardial function, respectively (Fig 3.3.2). In the ISO group there was a significant reduction in the FS_{end} when compared to the CONT (CONT, 44.21±1.19 vs. ISO, 37.40±0.80; p=0.0001), MET (MET, 45.88±1.54 vs. ISO, 37.40±0.80; p=0.0001) and ISO+MET (ISO+MET, 47.28±1.33 vs. ISO, 37.40±0.80; p=0.0001) groups. There was also a

significant reduction in the FS_{mid} in the ISO group when compared to the ISO+MET group (ISO+MET, 28.94±1.01 vs. ISO, 23.45±0.97; p=0.0339). Therefore isoproterenol induced left ventricular dysfunction and the administration of metformin improved midwall fractional shortening and improved left ventricular dilatation and dysfunction when co-administered with isoproterenol. Ejection fraction in the ISO group was significantly reduced when compared to the CONT (CONT, 44.2±1.19 vs. ISO, 37.40±0.80; p=0.0001), MET (MET, 45.88±1.54 vs. ISO, 37.40±0.80; p=0.0001) and ISO+MET (ISO+MET, 47.28±1.33 vs. ISO, 37.40±0.80; p=0.0001) groups. The administration of isoproterenol for seven months impaired the ability of the heart to eject blood from the ventricles and due to the lowered ejection fraction, showed evidence of heart failure.

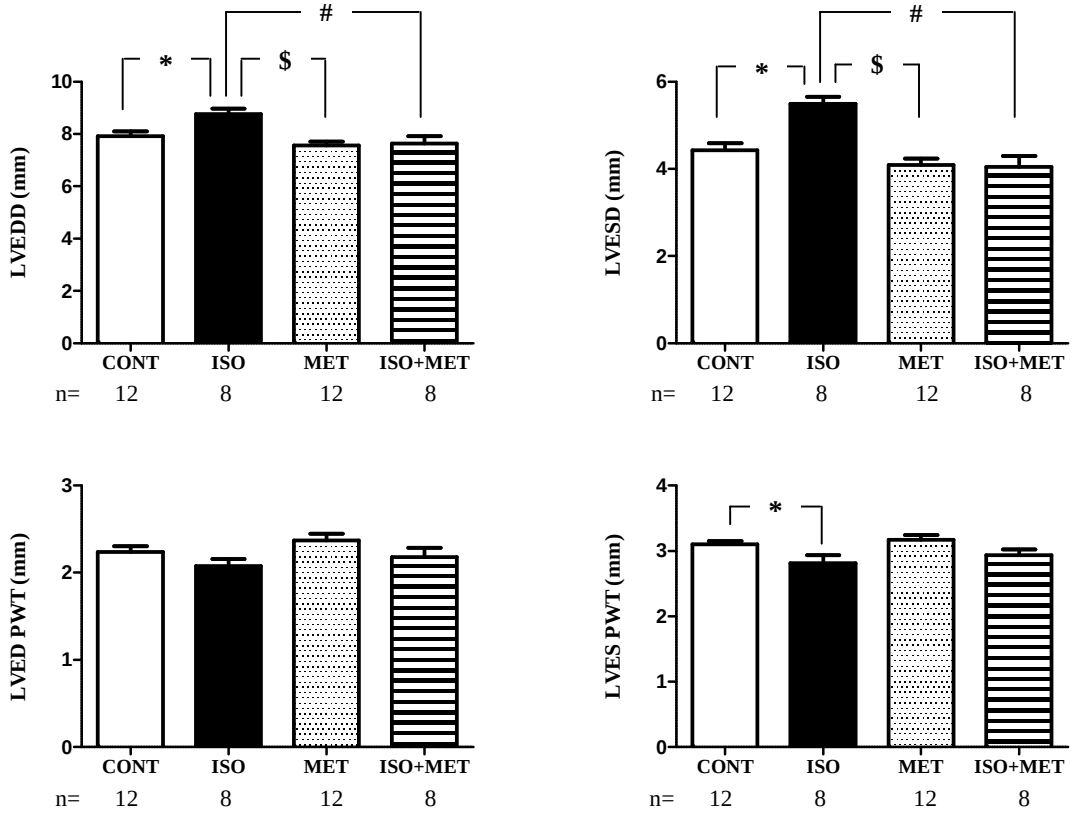

Figure 3.3.1 Chronic administration of isoproterenol induces left ventricular dilatation and dysfunction. Echocardiographic measurements were taken, following seven months of treatment with isoproterenol and metformin, and used to assess the cardiac dimension. LVEDD = left ventricular end-diastolic diameter, LVESD = left ventricular end-systolic diameter, LVED PWT = left ventricular end-diastolic posterior wall thickness, LVES PWT = left ventricular end-systolic posterior wall thickness. CONT = control, ISO = isoproterenol, MET = metformin, ISO+MET = isoproterenol+metformin.. Values are represented as means±SEM and were analysed using one-way ANOVA with Tukey *post hoc* test. *****$p < 0.05$ versus CONT, $^{\$}p < 0.05$ versus MET, $^{\#}p < 0.05$ versus ISO+MET.

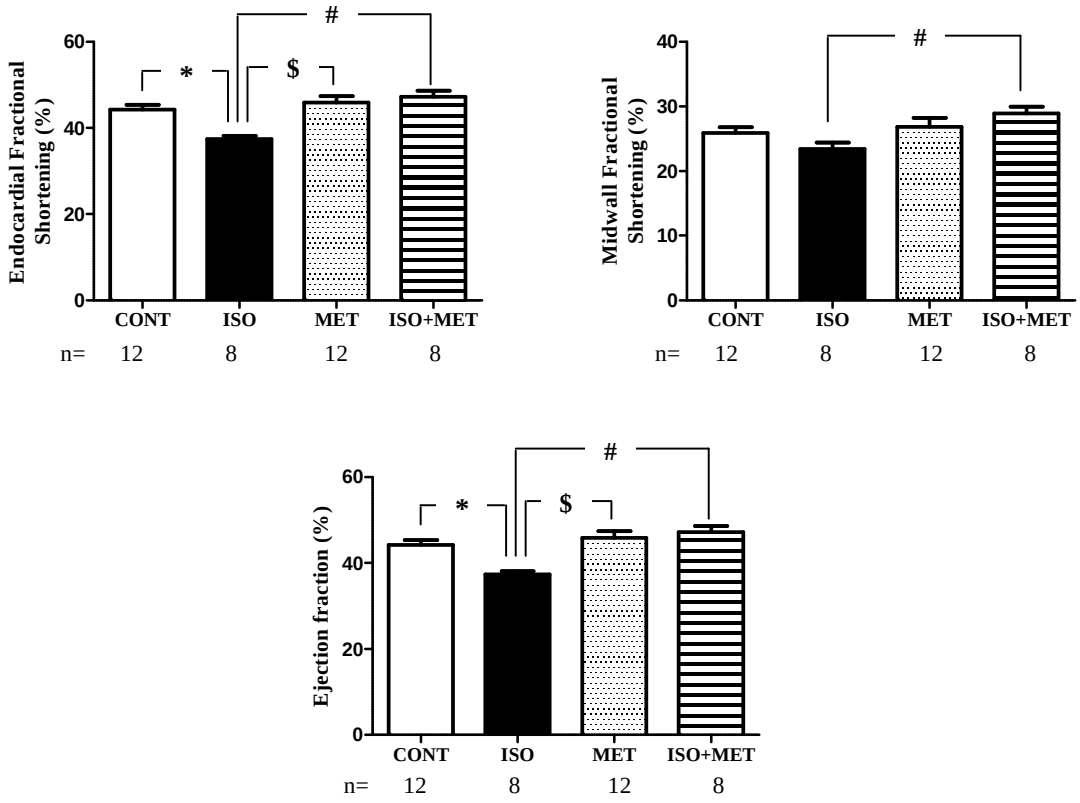

Figure 3.3.2 Chronic metformin co-administration prevents isoproterenol-induced left ventricular dilatation and pump dysfunction. Echocardiographic measurements were taken, following seven months of treatment with isoproterenol and metformin, and used to assess the cardiac function. CONT = control, MET = metformin, ISO = isoproterenol, ISO+MET = isoproterenol+metformin. Values are represented as means±SEM and were analysed using one-way ANOVA with Tukey *post hoc* test. *****$p < 0.05$ versus CONT, $^{\$}p < 0.05$ versus MET, $^{\#}p < 0.05$ versus ISO+MET.

3.4 Chronic administration of isoproterenol alters mitochondrial and myofibril ultrastructure in the myocardium.

To determine whether mitochondrial derangement occurred, relative mitochondrial area was calculated from the micrographs taken with the transmission electron microscope (see figure 3.4.1 and 3.4.2). Observations made using the electron micrographs showed that the CONT left ventricular cardiomyocytes had uniform interfibrillar spaces with linear mitochondrial arrangement and Z-band formation (Fig 3.4.1A). Whereas the ISO left ventricular cardiomyocytes had curved arrangement of the interfibrillar spaces in which the mitochondrial arrangement was irregular and the Z-band structure was visually thinner (Fig 3.4.1B). Also, the mitochondrial size and shape had increased and become rounder in the ISO sections (Fig 3.4.1B). The MET left ventricular cardiomyocytes showed linear mitochondrial arrangement of the interfibrillar spaces however the mitochondria were swollen (Fig 3.4.1C). The ISO+MET left ventricular cardiomyocytes showed an irregular mitochondrial arrangement. The mitochondria looked porous and almost ruptured with what looked liked cristae structures (Fig 3.4.1D). By visualisation we were able to observe the differences between the left ventricular ultrastructure of the various groups. However, quantified analysis of the relative mitochondrial area confirmed that chronic administration of isoproterenol significantly reduced the relative mitochondrial area when compared to the CONT group (CONT, 37.66±2.19 vs. ISO, 28.06±2.85; $p=0.05$).

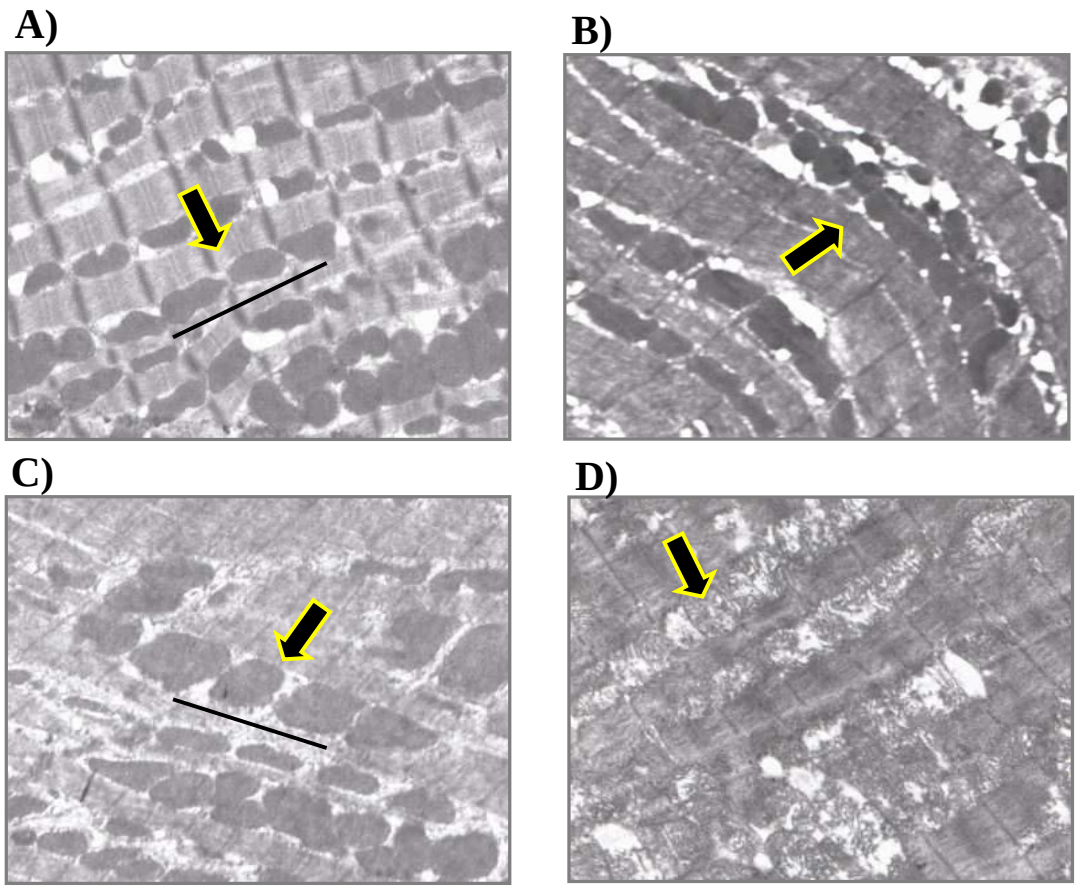

Fig 3.4.1 Chronic administration of isoproterenol alters mitochondrial and myofibril arrangement. Representative electron micrographs of longitudinal sections (x5000) of left ventricular tissue. A) Control; B) Isoproterenol, C) Metformin, D) Isoproterenol+Metformin. The arrow on A and C indicate linear arrangement of the interfibrillar space. The arrows on B and D indicate dearrangment of the mitochondria in the interfibrillar space.

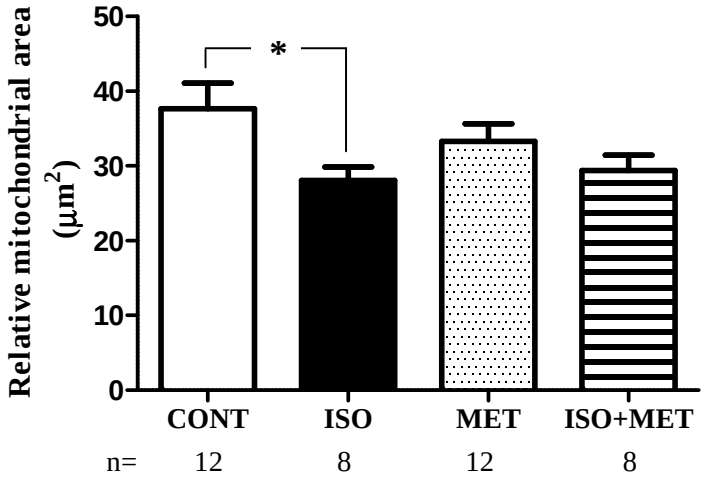

Figure 3.4.2 Chronic administration of isoproterenol alters mitochondrial area and arrangement in the myocardium. Micrographs obtained from transmission electron microscopy were used to assess relative mitochondrial area (μm^2) which determined the presence of mitochondrial ultrastructure derangement. CONT = control, MET = metformin, ISO = isoproterenol, ISO+MET = isoproterenol+metformin. Values are represented as means±SEM and were analysed using one-way ANOVA with Tukey *post hoc* test. *****$p < 0.05$ versus CONT.

3.5 Impact of chronic isoproterenol and metformin administration on metabolic transcriptional gene regulation.

Figure 3.5 shows the effect of chronic isoproterenol and metformin administration on genes regulating myocardial metabolism. Chronic isoproterenol and metformin administration produced no statistically significant effect on transcriptional gene regulation (Figure 3.5). Therefore, after seven months of treatment with isoproterenol and metformin the activity of the genes which regulate myocardial metabolism remained unchanged.

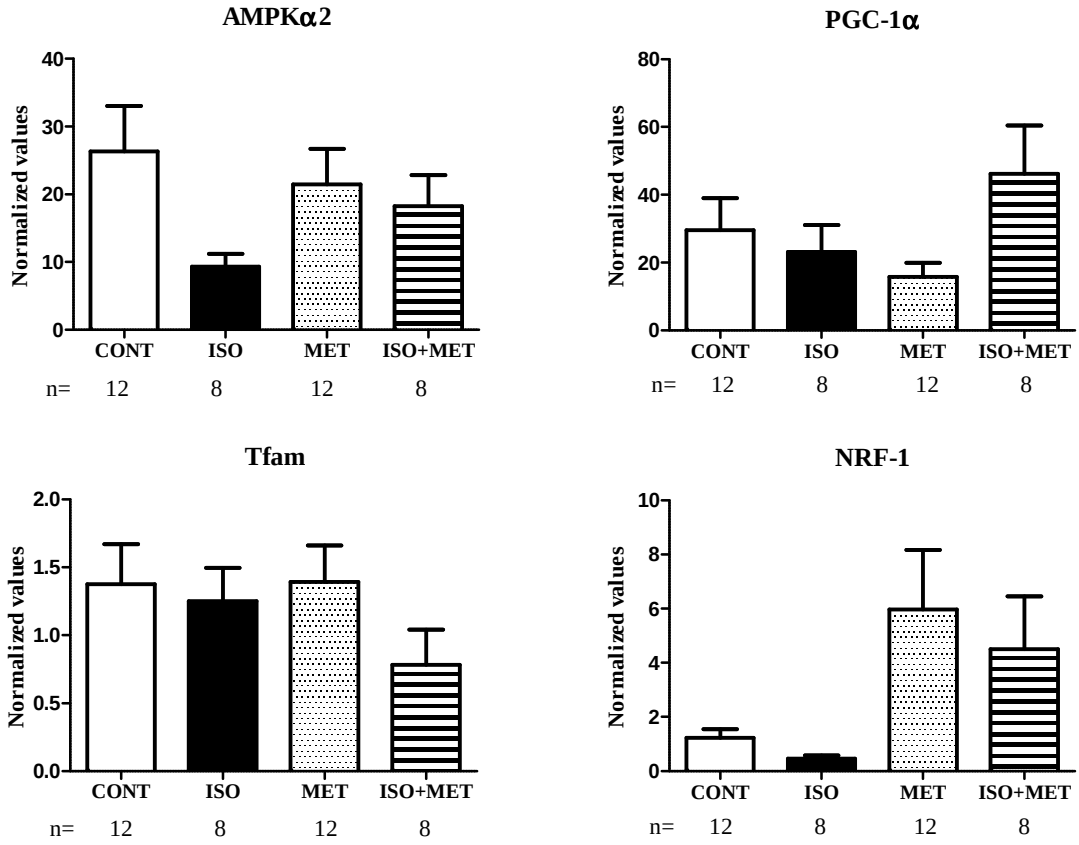

Figure 3.5 Impact of chronic isoproterenol and metformin administration on metabolic transcriptional gene regulation. Real-time PCR was used to assess transcript gene expression following seven months of treatment with isoproterenol and metformin. CONT = control, MET = metformin, ISO = isoproterenol, ISO+MET = isoproterenol+metformin. Values are represented as means±SEM and were analysed using one-way ANOVA with Tukey *post hoc* test.

Chapter 4

Discussion and Conclusion

4.1 The Main Findings of the Study.

We have shown that seven months of chronic adrenergic stimulation with isoproterenol induces left ventricular dilatation and pump dysfunction, as well as cardiac mitochondrial architectural derangement in male Sprague-Dawley rats. Surprisingly, following chronic adrenergic stimulation with isoproterenol, we did not observe any changes in total heart and left ventricular masses. Chronic administration of isoproterenol did not have a significant effect on body mass, bone growth, fasting plasma blood-glucose and triglyceride levels. Chronic isoproterenol administration induced mitochondrial and myofibril architecture derangement. However, no significant changes were shown in gene expression of metabolic and mitochondrial transcripts such as AMPKα_2, PGC-1α, NRF-1 and Tfam. Chronic co-administration of the metabolic modulator, metformin, decreased the final body mass, body mass gain and fasting plasma blood glucose levels. Chronic metformin administration did not alter metabolic and mitochondrial transcripts in isoproterenol-induced left ventricular dilatation and pump dysfunction. However, chronic co-administration of metformin prevented chronic adrenergic-induced left ventricular dilatation and pump dysfunction and retained cardiac mitochondrial architectural arrangement.

4.2 The Effect of Pharmacological Interventions on Body Mass and Metabolic Profiles.

In this study a beta-adrenergic agonist, isoproterenol, and a metabolic modulator, metformin, were chronically administered to male Sprague-Dawley rats. After seven months of treatment, the administration of isoproterenol and metformin alone did not change the final body mass of the animals in these groups. However, the co-administration of metformin with isoproterenol

reduced final body mass. The body mass gain remained unchanged in the groups that were administered isoproterenol and metformin alone; however, the co-administration of metformin with isoproterenol reduced body mass gain. A recent study which investigated reverse chamber remodeling following adrenergic-induced advanced cardiac dilatation and pump dysfunction in Sprague-Dawley rats (Booysen *et al*., 2012), reported that the administration of isoproterenol for six months did not alter the body weight in this model of heart failure. Another study investigating progressive ventricular remodeling in response to diffuse isoproterenol-induced myocardial necrosis in rats at two, six and 16 weeks also showed no changes in body weight (Teerlink *et al*., 1994). The evidence presented by both these studies is in agreement with our study in that the administration of isoproterenol alone does not affect growth. Our study is the first to investigate chronic administration of metformin in conjunction with chronic adrenergic-induced left ventricular dilatation and pump dysfunction. However, a study has shown that the chronic (four months) administration of metformin to non-diabetic insulin resistant chronic heart failure patients results in weight loss (Wong *et al*., 2012). Therefore, we can only speculate that the reduction in body mass and body mass gain brought about by chronic co-administration of metformin in this model is due to the weight loss effects of metformin, however future studies need to be done.

In the present study fasting blood glucose and triglyceride levels were measured in chronic adrenergic-induced left ventricular dilatation and pump dysfunction. Although there was no change in fasting blood glucose and triglyceride levels, chronic co-administration of metformin reduced the fasting blood glucose and did not have any impact on the triglyceride levels. The development of cardiac hypertrophy that accompanies isoproterenol

administration is reported to reduce fatty acid oxidation and reduce GLUT4 uptake thus reducing glycolysis (Heather *et al*., 2009; Bugger *et al*., 2010). The administration of metformin is known to activate AMPK which then promotes glycolysis (Gundewar *et al*., 2009; Turdi *et al*., 2010; Cittadini *et al*., 2011; Messaoudi *et al*., 2011; Xie *et al*., 2011;Yin *et al*., 2011; Wang *et al*., 2011). Although literature provides evidence that metformin has glucose lowering properties, in cases such as diabetes (Gundewar *et al*., 2009). The present study did not show any significant decrease in fasting blood glucose when metformin was administered alone. We speculate that the decrease in fasting blood glucose seen when metformin was co-administered with isoproterenol is due to a synergistic effect of the two drugs on glucose uptake hence lowering the circulating glucose levels however future investigation needs to be conducted.

4.3 Isoproterenol-Induced LV Dilatation and Pump Dysfunction.

Increased activity of the sympathetic nervous system is involved in cardiac hypertrophy and the development of heart failure (Triposkiadis *et al*., 2009; Parati & Esler, 2012). Data from a previous study has shown that an increase in plasma levels of catecholamines is associated with the development of myocardial hypertrophy (Taimor *et al*., 2001). Catecholamines are known to directly increase the activity of the sympathetic nervous system through the activation of beta-adrenoreceptors, which have been linked to the development of cardiac hypertrophy and heart failure (Taimor *et al*., 2001). Acute hyperadrenergic stimulation induces compensatory responses that assist in maintaining the homeostasis of the myocardium whereas the long-term effects of hyperadrenergic stimulation has deleterious effects that lead

to the progression of heart failure (Watson & May, 2006; Triposkiadis *et al*., 2009). Seven day administration of isoproterenol at 4.2 mg/kg/day activates the sympathetic nervous system in rats and as a result heart rate, plasma angiotensin II concentration and LV weight are increased (Nagano *et al*., 1992). A study investigating two and seven day isoproterenol administration have reported an increase in heart rate, reduced diastolic blood pressure, an increase in both right and left ventricular weights and total collagen as well as an association with persistent activation of circulatory renin-angiotensin system (Leenen *et al*., 2001). The administration of low dose isoproterenol for three months in rats led to the development of left ventricular pump failure which was associated with left ventricular dilatation with the presence of apoptosis and absence of intrinsic myocardial systolic failure and necrosis (Osadchii *et al*., 2007). Necrosis was evident in a study which investigated two week isoproterenol administration (Teerlink *et al*., 1994). All these studies have shown that isoproterenol administration activates the sympathetic nervous system, and is involved in left ventricular structural remodeling resulting in pump dysfunction and ultimately progressing to heart failure.

Studies that have investigated adrenergic-induced cardiac hypertrophy or cardiac dilatation and pump dysfunction using isoproterenol have all adjusted heart weight or left ventricular weight to body weight as an index of ventricular remodeling (Grimm *et al*., 1998; Osadchii *et al*., 2006; Osadchii *et al*., 2007; Osadchii *et al*., 2007; Kralova *et al*., 2008; Galindo *et al*., 2009; Mikusova *et al*., 2009; Yin et al., 2011; Booysen *et al*., 2012). Studies investigating pressure-overload-induced left ventricular hypertrophy (LVH) have also adjusted heart weight

and left ventricular weight to body weight as an index of ventricular remodeling (Allard *et al*., 1994; Dunn *et al*., 2011).

In contrast, a study which investigated proteomic remodeling of mitochondrial oxidative pathways in pressure overload-induced cardiac hypertrophy in Sprague-Dawley rats for 20 weeks, adjusted heart weight to tibial length as an index of cardiac hypertrophy (Bugger *et al*., 2010). Yin and colleagues (1982) have suggested that the use of heart weight to body weight ratios may be misleading indices to assess the degree or presence of hypertrophy because if the intervention in a study alters the body weight then an increase in heart weight to body weight ratio would be as a result of a decrease in body weight brought about by the intervention and therefore would not be as accurate as adjusting for tibia length, which reflects the relative lean body size throughout life. Consequently, a study investigating transcriptional profiling in isoproterenol-induced cardiomyopathy in rats over 10 days demonstrated the heart weight adjusted to tibial length was similar to the results found when heart weight was adjusted to body weight (Galindo *et al*., 2009). In the present study the heart weight and left ventricular (LV) weight was adjusted for tibial length and both these indices showed no change in the size of the heart which would be indicative of cardiac remodeling.

Most studies investigating cardiac hypertrophy and heart failure have demonstrated cardiac remodeling as a result of changes in muscle mass, size and shape of the heart which ultimately affects the overall function of the heart (Grimm *et al*., 1998; Leenen *et al*., 2001; Leong *et al*., 2002; Kralova *et al*., 2008; Mikusova *et al*., 2009; Dunn *et al*., 2011). A study investigating the effects of isoproterenol-induced cardiac hypertrophy in Wistar rats reported an increase in LV weight, LV weight/body weight ratio and increases in LV dimension (Mikusova *et al*.,

2009). A study which involved 3-6 weeks of pressure overload-induced hypertrophy, in mice, reported a decline in body weight and increase in heart weight (Dunn *et al*., 2011). Another study involving pressure overload-induced hypertrophy in Sprague-Dawley rats also confirmed increases in heart weight after eight weeks (Leong *et al*., 2002). These studies were all acute procedures and the increases in weights attributed to heart enlargement and LVH. In acute studies looking at isoproterenol-induced cardiac hypertrophy, body weight was reduced and heart weight was increased (Kralova *et al*., 2008; Leenen *et al*., 2001 & Grimm *et al*., 1998). A study by Allard and colleagues (1994), reported no change in final body weight and an increase in heart weight in Wistar-Kyoto rats with pressure-overload induced cardiac hypertrophy. From these studies it can be concluded that there is no association between body weight and heart weight within the various models regardless of the length of the study.

The impact of chronic isoproterenol administration on neurotensin-induced myocardial effects in rats was investigated for one month and showed no change in body weight but an increase in heart weight to body weight ratio as well as an increase in left ventricular weight to body weight ratio, therefore indicating the presence of cardiac hypertrophy (Osadchii *et al*., 2007). Booysen and colleagues (2012) have also shown no change in final body weight and an increase in heart weight, left ventricular and right ventricular weights, when adjusted for body weight, after six months of isoproterenol administration. These studies are from our laboratory and both demonstrate that body weight does not change with chronic administration of isoproterenol and by adjusting heart weight to body weight; cardiac hypertrophy can be assessed in the isoproterenol-model of cardiac dilatation and pump dysfunction. Although adjusting heart weight or left ventricular weight to body weight is a

common method for assessing left ventricular hypertrophy; this study showed no changes in heart weight and left ventricular weight across all groups therefore we cannot conclude that adjusting for tibial length would be an inaccurate measure for left ventricular hypertrophy in this model.

Not only does acute and chronic β-adrenergic stimulation induce left ventricular hypertrophy but various cardiac alterations which include myocyte degeneration, dilatation, apoptosis, necrosis, fibrosis and collagen changes are also present (Teerlink *et al*., 1994; Grimm *et al*., 1998; Shizukuda *et al*., 1998; Woodiwiss *et al*., 2001; Osadchii *et al*., 2007; Galindo *et al*., 2009). A study investigating transcriptional profiling in isoproterenol-induced cardiomyopathy compared to exercise-induced cardiac hypertrophy demonstrated that following 10 days of isoproterenol administration an increase in myocyte size, cardiomyocyte number and fibrosis contributed to the maladaptive increase in heart size present in pathological hypertrophy (Galindo *et al*., 2009). Chronic activation of the sympathetic nervous system via stimulation of β-adrenergic receptors contributes to dysregulation of myocardial growth under pathological conditions thus promoting myocardial apoptotic cell death and necrotic tissue scarring (Teerlink *et al*., 1994; Taimor *et al*., 2001; Osadchii *et al*., 2007).

Cardiac enlargement was evident following the administration of 150 mg/kg of isoproterenol in the development of cardiac hypertrophy and histological examination revealed lesions throughout the left and right ventricles with necrotic scarring (Grimm *et al*., 1998). A study done by Woodiwiss and colleagues (2001), has reported that seven months of isoproterenol administration and 20 weeks of pressure-overload hypertrophy in Sprague-Dawley rats,

reduces myocardial cross-linked collagen relative to non-cross linked collagen and this contributes to matrix disorganisation and LV dilatation. These studies all show that with the administration of isoproterenol, whether acute or chronic, there are many contributing mechanisms that can be linked to LV remodeling, such as cellular apoptosis, necrosis, collagen cross-linking and myocyte degeneration in the heart. Also, it has been reported that the generation of reactive oxygen species can have toxic effects on the myocardium of the heart and result in dysfunctional mitochondria which contribute to impaired cardiac structure and function that play a role in the development of heart failure (Hill & Singal, 1996; Sawyer & Colucci, 2000; Ide *et al*., 2001; Tsutsui *et al*., 2006; Kim *et al*., 2008). A study investigating pressure-overload-induced hypertrophy in mice for four weeks demonstrated an increase in ROS production which was associated with mitochondrial damage and dysfunction and was characterised by an increase in lipid peroxidation, a decrease in mitochondrial RNA transcripts and low electron transport complex enzyme activity (Ide *et al*., 2001). Most of the studies mentioned all link impaired cardiac structure and function to dysfunctional mitochondria and left ventricular remodeling.

In the present study, we did not investigate the impact of apoptosis, necrosis and cardiac contractility on left ventricular remodeling in the isoproterenol-model of heart failure. However, future investigation of the mechanisms through which these variables act would be helpful in understanding how myocardial changes take place in the isoproterenol-model of heart failure. Nevertheless, using echocardiography, we assessed whether chronic administration of isoproterenol for seven months would result in changes in cardiac dimension thus contributing to reduced function of the heart. The present study shows that

although there was no change in the heart size following seven months of treatment with low dose isoproterenol, there was an increase in LVEDD and LVESD and a decrease in FS_{end} resulting in cardiac dilatation and pump dysfunction. In our laboratory we have previously shown that daily administration of low dose isoproterenol for six months induces myocardial apoptosis, cardiac dilatation (as indexed by increased LVEDD), pump dysfunction (as indexed by decreased LV FS_{end}) and decreased cardiac contractility (Booysen *et al*., 2012).

Although the models of heart failure induced in animal models vary, we were able to confirm that isoproterenol administration for seven months results in chronic adrenergic-induced left ventricular dilatation and pump dysfunction and this is in agreement with previous studies (Osadchii *et al*., 2006; Osadchii *et al*., 2007; Booysen *et al*., 2012). Studies investigating pressure overload-induced heart failure and volume overload-induced heart failure in rats following 20-21 weeks all confirmed an increase in LVEDD and LVESD and a reduction in FSend (Norton *et al*., 2002; Benes *et al*., 2011; Bugger *et al*., 2012). Although the models of heart failure presented by these studies were not the same, similarities exist in cardiac functional changes regardless of the origin of the heart failure. To further investigate how the chronic adrenergic-induced heart failure model differs from various other animal models such as volume and pressure overload-induced heart failure, mitochondrial and myofibril architecture was examined to see if the extent of damage brought about by the failing myocardium differs between models and if the evidence found contributes to the changes in the left ventricular function.

4.4 Chronic Administration of Isoproterenol Disturbs Mitochondrial and Myofibril Architectural Arrangement.

In our study, the quantitative analysis of the left ventricular tissue confirmed that chronic adrenergic stimulation, via the administration of isoproterenol, decreased the area inhabited by the mitochondria. Visual observation of the electron micrographs for the control group demonstrated prominent Z-bands with linear arrangement and uniform shaped mitochondria. However, the group of animals administered isoproterenol, demonstrated Z-band derangement and smaller, irregular shaped mitochondria with a partly linear and curved arrangement. In a seven day isoproterenol adrenergic-induced hypertrophy study, electron microscopy showed changes in mitochondrial size and shape with slight myofibril splitting, irregular z discs and contracted sarcomeres, which ultimately led to mitochondrial architectural disorganisation (Mikusova *et al*., 2009).

In contrast, a study investigating pressure overload-induced hypertrophy over a period of 20 weeks demonstrated cristae derangement and reduced cristae density in the failing heart, also stereological quantification demonstrated reduced mitochondrial volume density (Bugger *et al*., 2010). Another pressure overload-induced hypertrophy study carried out for six weeks demonstrated that in the presence of left ventricular hypertrophy abnormalities of the myocardium and derangement of myofibrils and Z-bands exist (Dunn *et al*., 2011). According to Dhalla and colleagues (1996), characteristics of pressure overload-induced hypertrophy include: a decline in myocardial function, thinning of the left ventricular wall and changes within the ultrastruture of the mitochondria. All these studies confirm that with pressure overload-induced hypertrophy derangement of the mitochondria and myofibrils are present

and may lead to the dysfunction which is present in this model. On the other hand, a study investigating volume-overload induced hypertrophy in rats demonstrated no structural abnormalities in the myofibrils and the mitochondria (Benes *et al*., 2011).

Even though, the evidence to support cardiac dilatation and pump dysfunction in chronic adrenergic-, pressure overload- and volume overload-induced models are similar, the mechanisms involved in the development of these functional changes are not the same. This can be confirmed by the lack of change in mitochondrial and myofibril architecture in the volume overload-induced model compared to the pressure overload and isoproterenol models. Excessive generation of reactive oxygen species is detrimental to the functional integrity of the myocardium (Ide *et al*., 1999). Perhaps the presence of reactive oxygen species generation in this model of heart failure would result in derangement in the mitochondrial and myofibril architecture. The mechanisms involved in the observed functional changes seem to be specific to the individual animal models of heart failure investigated and whether the presence of reactive oxygen species in the models cause changes in the mitochondrial and myofibril ultrastructure are unknown. Therefore in future studies reactive oxygen species levels should be monitored and overall cardiac function and the actual metabolic transcriptional role of the mitochondria should be assessed to assist in differentiating between the models.

4.5 Metformin Prevents Isoproterenol-Induced LV Dilatation and Pump Dysfunction.

The present study is the first to provide clear evidence that the administration of metformin provides cardioprotection by preventing LV dilatation and dysfunction in chronic adrenergic isoproterenol-induced heart failure by reducing LVEDD and LVESD and increasing FS_{end}.

However, a study which investigated the acute effects of metformin on isoproterenol-induced cardiac hypertrophy over a one week period was the first of its kind to report that co-administration of metformin reduces heart weight and left ventricular posterior wall thickness and therefore partially inhibits isoproterenol-induced cardiac hypertrophy (Cha *et al*., 2010). Unlike the present study where the effects of chronic metformin administration were observed in chronic adrenergic-induced heart failure, previous studies have focused on the cardioprotective effects of metformin on the acute adrenergic model and volume-overload-induced cardiac hypertrophy (Gundewar *et al*., 2009; Benes *et al*., 2012). With one study to date, that observed the effects of metformin in cardiac dilatation and pump dysfunction over 12 months in a pressure-overload model of heart failure (Cittadini *et al*., 2011).

Clinically, metformin is prescribed as an anti-diabetic drug and the cardioprotective properties are attributed to its ability to lower blood glucose (Kirpichnikov *et al*., 2002; Messaoudi *et al*., 2011). A pre-clinical study involving chronic metformin administration, for 12 months, to spontaneously hypertensive rats shows evidence that metformin prevents LV remodeling by reducing LV dilatation and wall stress and improves systolic and diastolic function by restoring myocardial contractile reserves and myocardial efficiency (Cittadini *et al*., 2011). The study by Cittadini and colleagues (2011) was the first of its kind to investigate the effects of metformin in an animal model of pressure overload-induced heart failure over a 12 month period. Another study (Yin *et al*., 2012) observing chronic administration of metformin for 12 weeks, in a non-diabetic rat model of post myocardial infarction, demonstrated that metformin exerts cardioprotective effects on LV remodeling via a reduction in necrosis and apoptosis which results in a decrease in the myocardial size; as well as a reduced LV dilatation and

dysfunction as a result of reduced left intraventricular septum diastolic and systolic diameters. Furthermore another study investigating the effect of metformin administration, for four weeks, in an animal model of pressure-overload, reported a reduction in LVEDD and LVESD which is evidence of reduced dilatation in the heart (Wang *et al*., 2011). Another study investigating the effects of four week administration of metformin in pressure-overload-induced hypertrophy reported a 47% overall survival rate in mice as well as a 28% significant improvement in LVEDD and LVESD therefore improving cardiac remodeling and function during (Gundewar *et al*., 2009). These studies all demonstrate that in models of pressure overload-induced hypertrophy, metformin has cardiac protective properties against LV remodeling

In contrast, a study which investigated the effect of metformin administered for 21 weeks on cardiac function in a volume-overload model of hypertrophy, in rats, reported that metformin did not improve systolic or diastolic pressures nor did metformin improve LVEDD and LVESD (Benes *et al*., 2011). Therefore, studies which have focused on the effects of metformin on pressure-overload-induced hypertrophy and cardiac dilatation and pump dysfunction are in agreement that metformin exerts cardiac protective effects against LV remodeling (Cittadini *et al*., 2011; Wang et al., 2011; Yin *et al*., 2011) compared to the lack of cardioprotective effects of metformin in the volume-overload model of hypertrophy (Benes *et al*., 2011).

The acute adrenergic stimulation model of cardiac hypertrophy used a 150 mg/kg/day dose of metformin (Cha et al., 2010) and studies investigating pressure-overload induced hypertrophy or heart failure and the effects of metformin used doses of 125 µg/kg/day, 100 mg/kg/day and

250 mg/kg/day of metformin (Gundewar *et al*., 2009; Cittadini *et al*., 2011; Wang *et al*., 2011; Yin *et al*., 2011). All these studies showed that regardless of the dose used, LV remodeling can be prevented in acute adrenergic stimulation and pressure-overload-induced hypertrophy and heart failure. Whereas a study investigating the effects of 300 mg/kg/day dose of metformin on volume-overload-induced heart failure lacks cardioprotection against LV remodeling (Benes *et al*., 2011). In contrast, we have shown that when a 300 mg/kg/day dose of metformin is administered, LV dilatation and pump dysfunction are prevented in a chronic adrenergic isoproterenol-induced model of heart failure. Therefore, the effects of metformin are dependent on the type of heart failure model present and regardless of the dose of metformin administered, whether in pressure-overload or chronic adrenergic stimulation models, cardioprotection is exerted against LV dilatation and pump dysfunction. This raises the question as to whether chronic administration of metformin will induce metabolic and mitochondrial architectural changes in the chronic adrenergic model of heart failure and if these changes are model dependent.

4.6 Metformin Retains Mitochondrial and Myofibril Architecture Arrangement.

Until recently little was known about the effects of metformin on mitochondrial ultrastructure in animal models of heart failure, using electron transmission microscopy. The present study is the first to observe the effects of chronic metformin administration on mitochondrial and myofibrillar architecture in chronic adrenergic-induced cardiac dilatation and pump dysfunction. Statistically, no changes were seen in the mitochondrial and myofibrillar architecture when metformin was chronically administered in conjunction with the

isoproterenol-induced model of heart failure. However through visual observation, mitochondrial arrangement remained linear but the mitochondria appeared porous and ruptured with cristae evident. With chronic administration of metformin alone, visual observations showed mitochondria which were rounder and fuller in shape, whilst possessing a linear arrangement. Statistically, there was no evidence to support overall mitochondrial and myofibril ultrastructure change in metformin treated animals. A study investigating the effects of chronic metformin administration in rats with volume-overload-induced hypertrophy reported no statistical differences in mitochondrial ultrastructure morphology, however, visual observation of the electron micrograph representing this group showed a variety of round and irregular shaped mitochondria (Benes *et al.*, 2011).

A study which investigated the positive effects of metformin on cardiomyopathy induced by anthracycline antibiotic, doxorubicin, demonstrated that mitochondrial ultrastrutural changes are dependent on the dose of metformin administered (Ashour *et al.*, 2012). The study demonstrated that a 50mg/kg dose of metformin administered in doxorubicin-induced cardiomyopathy brought about a loss of myofibrils with evidence of mitochondrial size and shape variation, whereas the administration of 500mg/kg dose of metformin showed normal mitochondrial size and shape and normal cristae arrangement. Briefly, doxorubicin is administered to patients with breast cancer, childhood solid tumours, soft tissue sarcomas and aggressive lymphomas (Minotti *et al.*, 2004). However, clinically the administration of this anti-cancer drug causes cardiotoxicity which ultimately leads to chronic cardiomyopathies and congestive heart failure (Minotti *et al.*, 2004). According to the study done by Ashour and colleagues (2012), metformin administration in conjunction with doxorubicin-induced

cardiomyopathy demonstrated antioxidant activity as indicated by the reduction in glutathione levels. A study has also found that metformin inhibits mitochondrial respiration in hepatocytes via the indirect effect targeted on the respiratory chain complex I; however, the exact mechanism was speculated to act via a complex signaling pathway that interacts between the drug and a membrane receptor (El-Mir *et al*., 2000).

If metformin does possess both antioxidant properties as well as the ability to inhibit cellular respiration at the level of the respiratory chain complex I, then perhaps the lack of mitochondrial and myofibril architecture changes in the present study could be characteristic of these cardioprotective findings. However, to test this hypothesis, future studies would have to be carried out to investigate the impact of metformin on cellular respiration and oxidative stress in chronic-adrenergic-induced left ventricular dilatation and pump dysfunction. Perhaps the regulation of metabolic transcription genes could assist in understanding why the mitochondrial and myofibril architecture remains unchanged when metformin is administered in conjunction with this model.

4.7 Metabolic transcriptional gene regulation remains unchanged.

Data from the present study shows that metabolic transcriptional gene regulation is not altered when chronic adrenergic stimulation with isoproterenol induces cardiac dilatation and pump dysfunction, as well as mitochondrial and myofibril ultrastructure derangement. Animal and human studies have shown that a decrease in myocardial fatty acid oxidation is an independent predictor of pathological hypertrophy (de las Fuentes *et al*., 2003). In

pathological hypertrophy, energy metabolized by the heart is sourced from glycolysis rather than from fatty acid oxidation and if glycolysis is prolonged, such as the case in heart failure, this leads to mitochondrial dysregulation (Leong *et al*., 2002; Taegtmeyer, 2004). A study demonstrated that in a rat model of pressure-overload hypertrophy there were lower rates of fatty acid oxidation and higher rates of glycolysis, after an eight week period, therefore glucose oxidation was more energy efficient than fatty acid oxidation (Allard *et al*., 1994). Van Bilsen and colleagues (2009) have highlighted that the lack of oxygen or defects in mitochondrial substrate oxidation are responsible for inadequate ATP generation. All these studies show that cardiac stress remodels metabolism and leads to mitochondrial ATP deficiency and therefore mitochondrial dysfunction. In the pressure-overload model of LVH, glycolysis was markedly decreased at the six week mark after heart failure was established, and the increase in glycolysis in the LVH stage was characterised as adaptive metabolic remodeling (Dunn *et al*., 2011). Another study demonstrated that during decompensated heart failure, a change in substrate utilisation takes place in which fatty acid uptake is reduced and glucose utilisation increases (Recchia *et al*., 1998). In contrast, a study has shown that myocardial fatty acid oxidation is not altered in moderate severity ischemic induced-heart failure in dogs (Chandler *et al*., 2004). Although speculation exists as to whether glycolysis continues throughout heart failure, the exact mechanisms involved in metabolic remodeling in heart failure remain unknown.

Activation of the sympathetic nervous system and the presence of contractile dysfunction have been reported to be involved in the alteration of metabolism during heart failure (Ashrafian *et al*., 2007). Although glycolysis is present in pathological hypertrophy, which is

present in the development of heart failure, differences in metabolic remodeling exist in the various animal models. Studies have shown evidence to support that gene expression is associated with metabolic and structural remodeling therefore; transcriptional regulation should be assessed during the transition of hypertrophy to heart failure (Taimor *et al*., 2001; Kato *et al*., 2010). Perhaps metabolic alteration through sympathetic nervous system activation also plays a role in regulating transcriptional genes. However, future studies investigating the impact of sympathetic nervous system stimulation on the markers of metabolic regulation and the expression of transcriptional genes and protein would need to be done in this model.

AMPK is a key regulator of energy metabolism and studies have investigated the activity of AMPK in various models of cardiac hypertrophy (Allard *et al*., 2007; Zarrinpashneh *et al*., 2008). In pressure-overload hypertrophy elevated activity of AMPK indicates involvement in the alteration of glucose metabolism (Allard *et al*., 2007). A study demonstrated that seven days of isoproterenol treatment induces hypertrophy and there is no evidence to support an increase in AMPK activity. Therefore it has been suggested that the activation of AMPK seen during the hypertrophic response is more of an adaptive metabolic response (Zarrinpashneh *et al*., 2008). Although our study was in agreement with that of Zarrinpashneh and colleagues (2008), and there was no evidence to support an increase in AMPKα_2 expression in chronic adrenergic-induced cardiac dilatation and pump dysfunction, perhaps AMPKα_2 activity and expression was increased at a much earlier time point. Studies have also shown that the activation of AMPKα_2 in the heart is important to attenuate the development of cardiac hypertrophy (Zarrinpashneh *et al*., 2006; Li *et al*., 2007). The activity of AMPK seems to be

model dependent and AMPKα_2 expression is not seen in both acute and chronic adrenergic models of hypertrophy and heart failure. Therefore this does not rule out the occurrence of metabolic adaptation in this model as future studies need to be carried out.

AMPK is the metabolic modulator that regulates ATP levels in the myocardium by increasing either glucose or fatty acid metabolism to meet the cell's energy demand (Dyck & Lopaschuk, 2006). A study investigating the Dahl salt-sensitive model of heart failure for 6 weeks, reported a decrease in fatty acid uptake, an increase in glucose uptake, an increase in reactive oxygen species production and a decrease in expression of genes regulating fatty acid oxidation such as PGC-1α and NRF-1 (Kato *et al*., 2010). In pressure-overload-induced heart failure, a reduction in PGC-1α signaling has been reported to negatively impact the activity of the electron transport chain (Bugger *et al*., 2010). PGC-1α is the mediator that regulates the mitochondrial biogenesis cascade thereby increasing mitochondrial oxidative capacity, thus regulating cardiac fuel selection and ATP-producing capacity (Huss & Kelly, 2005). PGC-1α also induces mRNA for NRF-1 which is a regulator of Tfam (Wu *et al*., 1999). Another study has confirmed that Tfam regulates mitochondrial DNA copy number and is essential for mitochondrial biogenesis (Larsson *et al*., 1998). In summary, PGC-1α co-activates the genes involved in mitochondrial biogenesis and in doing so induces the activity of NRF-1 which in turn has a dual role in activating mitochondrial respiration and Tfam which regulates the production of new mitochondria.

A study has shown that in the failing heart an increase in the generation of reactive oxygen species occurs and mitochondrial damage and dysfunction can be characterised by a decrease in mtDNA and reduced activity in electron transport chain complex I (Ide *et al*., 1999 & Ide *et*

al., 2001). An increase in mitochondrial oxidative stress leading to a reduction in the quantity of mitochondria has been reported to reduce mitochondrial biogenesis during heart failure (Ren *et al*., 2010). Not only does the regulation of mitochondrial and transcriptional genes play a role in metabolic remodeling but gene expression is impacted by the presence of reactive oxygen species therefore the overall synthesis and function of the mitochondria are at risk. The present study showed no changes in transcriptional gene expression levels for AMPKα_2, PGC-1α, NRF-1 and Tfam after seven months of β-adrenergic receptor activation with isoproterenol. A study investigating acute β-adrenergic stimulation in young adult males reported no changes in mitochondrial protein synthesis and in mRNA gene expression for PGC-1α, Tfam and NRF-1 which are involved in mitochondrial biogenesis in skeletal muscle (Robinson *et al*., 2010). Their study (Robinson *et al*., 2010) demonstrated no changes in mRNA expression of PGC-1α, Tfam and NRF-1 in human men when administered isoproterenol for one hour. However, when using this method it was emphasised that the protein content and activity of the transcription factors is unknown and therefore serves as a limitation (Robinson *et al*., 2011; Wong & Medrano, 2005).

In contrast, the present study investigated mitochondrial cDNA gene expression of AMPKα_2, PGC-1α, NRF-1 and Tfam following seven months of chronic isoproterenol administration and found no changes in gene regulation that could indicate mitochondrial biogenesis. Although we did not detect changes in gene expression, the method which was used is reproducible and widely used (Wong & Medrano, 2005); however we cannot rule out the possibility that metabolic gene regulation may have been altered at some point in the experiment. Future studies could assist in understanding what happens to the transcription

factors as well as help identify the deleterious markers that are indicative of reactive oxygen species in the chronic isoproterenol model of cardiac dilatation and pump dysfunction.

A study using a pharmacological AMPK activator, AICAR demonstrated that increasing AMPKα_2 attenuates pressure overload-induced hypertrophy after 7 weeks in Sprague Dawley rats (Li *et al*., 2007). In the present study, chronic administration of metformin alone did not alter the expression of AMPKα_2, PGC-1α, NRF-1 or Tfam. However, the administration of metformin is known to activate AMPK and studies have confirmed cardioprotective effects (Gundewar *et al*., 2009; Turdi *et al*., 2010; Cittadini *et al*., 2011; Messaoudi *et al*., 2011; Xie *et al*., 2011;Yin *et al*., 2011; Wang *et al*., 2011).

The administration of metformin for 4 weeks promotes an increase in AMPKα_2 and PGC-1α in hypertrophy thus improving mitochondrial respiration and preventing mitochondrial dysfunction thus displaying cardioprotection (Gundewar *et al*., 2009). A study investigating the effects of metformin on cardiac function and survival in volume-overload induced hypertrophy reported that long term administration of metformin in this model, had no effect on AMPK activation and did not improve cardiac function (Benes *et al*., 2011). In a rat model of chronic heart failure, it has been reported that metformin prevents the progression of chronic heart failure with an increase in AMPK phosphorylation (Wang *et al*., 2011). Although the present study showed no expression changes for AMPKα_2, PGC-1α, NRF-1 and Tfam, when metformin was administered alone or co-administered with isoproterenol, in a future study protein expression should be investigated to assess the phosphorylation of the genes.

Previous studies have shown that the effects of metformin are dependent on the type of model investigated (Gundewar *et al*., 2009; Benes *et al*., 2011; Yin *et al*., 2011; Wang *et al*., 2011; Cittadini *et al*., 2012). A study investigating the effects of long-term metformin administration on the cardiac function and survival in a volume-overload model of heart failure reported no changes in myocardial AMPK, ATP content, mitochondrial function or morphology as well as no change in cardiac performance (Benes *et al*., 2011). Another study investigating the effects of metformin on isoproterenol-induced cardiac hypertrophy also reported no changes in AMPK activity (Cha *et al*., 2010). In the present study chronic co-administration of metformin with isoproterenol improved cardiac function and prevented cardiac dilatation and pump dysfunction as well as maintained mitochondria and myofibril architecture however metabolic and transcriptional gene expression was not altered and perhaps in this model of heart failure mitochondrial biogenesis does not occur. This study does confirm that chronic administration of the metabolic modulator, metformin, in chronic adrenergic stimulation does prevent left ventricular dilatation and pump dysfunction induced by isoproterenol administration.

4.8 Limitations and Future Studies.

When observing the metabolic gene transcript regulation, in the present study, we see large variations between the groups. These variations could possibly be corrected by increasing the sample size of each group whilst remaining within ethical boundaries of using as few animals as is reasonable possible. The duration of treatment administered to the animals was seven months; therefore it is possible that changes in gene expression could have occurred earlier in

the time course. Although the animals were fasted 16 hours prior to measuring fasting blood glucose and triglycerides all the animals could not be terminated all at once as the lab only has one qualified echocardiographer and the hearts had to be harvested fresh for gene expression and transmission electron microscopy. Moreover, the dose of anesthetic was calculated according to the average body mass of the animals however some animals took longer to be anaesthetised thus the dose of anaesthetic and the duration that the animals were anaesthetised for could have also contributed to the variation in metabolic gene transcript expression.

To assist in determining the efficiency of the mitochondria, mitochondrial functional studies were required. We used two kits namely, mitochondrial isolation kit and cytochrome c oxidase kit, to assist us in observing the mitochondrial function. Although we followed the manufacturer's manual, we were unable to obtain reproducible data using these kits.

With regards to mitochondrial and myofibril architecture architecture, more experience was needed when preparing the glass knives and cutting resin block sections as scoring was evident in some of the micrographs and these images had to be eliminated from the mitochondrial counting procedure.

With these limitations in mind, we propose future studies be done in which the investigation of metabolic changes and hemodynamic changes should be done separately thus eliminating any damage to the tissue that would be brought about by hemodynamic measurements as well as the effect of anaesthetic. With regards to mitochondrial function and reactive oxygen species, both the mitochondrial isolation kit and the cytochrome c oxidase kit should be optimised further otherwise alternate biochemical isolation protocols should be considered. Moreover, an acute study looking at *in vivo* and *ex vivo* adrenergic models should be carried

out in order to identify and understand the changes that occur in metabolic gene transcript expression when metformin and isoproterenol are co-administered.

4.9 Conclusion

In this study we confirmed that low dose administration of isoproterenol for seven months results in cardiac dilatation and pump dysfunction. Our findings suggest that the co-administration of metformin prevents cardiac dilatation and pump dysfunction that is seen in the isoproterenol model of heart failure. Chronic administration of isoproterenol altered mitochondrial and myofibril ultrastructure, however, co-administration of metformin prevented these changes. The data presented in this study are novel in showing that metformin provides cardiac protection in chronic adrenergic model of heart failure and although this study has not been able to identify the precise pathways involved in functional and metabolic remodeling, it serves as a platform for future investigation. Many animal models of heart failure have shown the cardiac protective qualities of metformin therefore clinically the administration of metformin should be considered beneficial in all patients with heart failure.

APPENDICES

APPENDIX A

Recipe for 10 X PBS – 1 Litre

Dissolve 80g NaCl, 2g KCl, 26.8g $Na_2HPO_4 – 7H_2O$ and 2.4g KH_2PO_4 in 800ml distilled H_2O

Adjust to pH 7.3 with HCl

Adjust volume to 1L with distilled H_2O

(To make up 1L 1 X PBS: add 100ml 10 X PBS to 900ml distilled H_2O)

Recipe for resin mix:

5.62g Araldite

7.75g Epon 812

15g DDSA

Mix well on rotating mixer

For use add accelerator

Add 0.71g DMP 30 (1:40)

APPENDIX B

AESC 3

UNIVERSITY OF THE WITWATERSRAND, JOHANNESBURG

STRICTLY CONFIDENTIAL

ANIMAL ETHICS SCREENING COMMITTEE (AESC)

CLEARANCE CERTIFICATE NO. 2010/27/04

APPLICANT: Ms V Peterson

SCHOOL: Physiology
DEPARTMENT:
LOCATION:

PROJECT TITLE: **Metformin, a metabolic modulator, corrects metabolic dysregulation and restores mitochondrial integrity in isoproterenol-induced left ventricular hypertrophy in Sprague Dawley rats**

Number and Species

45 Sprague Dawley rats

Approval was given for the use of animals for the project described above at an AESC meeting held on 04.05.2010. This approval remains valid until 04.05.2012

The use of these animals is subject to AESC guidelines for the use and care of animals, is limited to the procedures described in the application form and to the following additional conditions:

Saline needs to be given for 2 weeks prior to starting the isoproterenol injections to habituate rats to the animal handling and the procedure.
The volume of the saline and isoproterenol injections should be 0.1 mls per injection.

Signed: _____ NORTON _____ Date: 31/05/2010
(Chairperson, AESC)

I am satisfied that the persons listed in this application are competent to perform the procedures therein, in terms of Section 23 (1) (c) of the Veterinary and Para-Veterinary Professions Act (19 of 1982)

Signed: _____ Date: 31/05/2010
(Registered Veterinarian)

cc: Supervisor:
Director: CAS

Works 2000/lain0015/AESCCert.wps

REFERENCES

REFERENCES

1. Abassi Z, Goltsman I, Karram T, Winaver J and Hoffman A. (2011). Aortocaval fistula in rat: a unique model of volume-overload congestive heart failure and cardiac hypertrophy. *J Biomed Biotechnol* doi:10.1155/2011/729497.

2. Allard MF, Parsons HL, Saeedi R, Wambolt RB and Brownsey R. (2007). AMPK and metabolic adaptation by the heart to pressure overload. *Am J Physiol Heart Circ Physiol* **292**, H140-H148.

3. Allard MF, Schonekess BO, Henning SL, English DR and Lopaschuk GD. (1994). Contribution of oxidative metabolism and glycolysis to ATP production in hypertrophied hearts. *Am J Physiol* **267**, H742-H750.

4. Andersson DC, Fauconnier J, Yamada T, Lacampagne A, Zhang S, Katz A and Wasterblad H. (2011). Mitochondrial production of reactive oxygen species contributes to the β-adrenergic stimulation of mouse cardiomyocytes. *J Physiol* **589**, 1791-1801.

5. Arad M, Seidman CE and Seidman JG. (2007). AMP-activated protein kinase in the heart: role during health and dieseas. *Circ Res* **100**, 474-488.

6. Ashour AE, Sayed-Ahmed MM, Abd-Allah AR, Korashy HM, Maayeh ZH, Alkhalidi H, Mubarak M and Alhaider Abduqader. (2012). Metformin rescues the myocardium from doxorubicin-induced energy starvation and mitochondrial damage in rats. *Oxid Med Cell Longev* doi:10.1155/2012/434195.

7. Ashrafian H, Frenneaux MP and Opie LH. (2007). Metabolic mechanisms in heart failure. *Circulation* **116**, 434-448.

8. Badeer HS. (1964). The biological significance of cardiac hypertrophy. *Am J Cardiol* **14**, 133-138.

9. Benes J, Kazadova L, Drahota Z, Houstek J, Medrikovas D, Kopecky J, Kovarova N, Vrbacky M, Sedmera D, Strnad H, Kolar M, Petrak J, Benada O, Skaroupkova P, Cervenka L and Melenovsky V. (2011). Effect of metformin therapy on cardiac function and revival in a volume-overload model of heart failure in rats. *Clin Sci* **121**, 29-41.

10. Bergeron R, Ren JM, Cadman KS, Moore IK, Perret P, Pypaert M, Young LH, Semenkovich CF and Shulman GI. (2001). Chronic activation of AMP kinase results in NRF-1 activation and mitochondrial biogenesis. *Am J Physiol Endocrinol Metab* **281**, E1340-E1346.

11. Bernstein D, Fajardo G and Zhao M. (2011). The role of β-adrenergic receptors in heart failure: differential regulation of cardiotoxicity and cardioprotection. *Prog Pediatr Cardiol* **31**, 35-38.

12. Booysen HL, Norton GA, Opie LH and Woodiwiss AJ. (2012). Reverse chamber remodelling following adrenergic-induced advanced cardiac dilatation and pump dysfunction. *Basic Res Cardiol* doi: 10.1007/s00395-011-0238-0.

13. Braunwald E. (2001). Expanding indicator for beta-blockers in heart failure. *N Engl J Med* **344**, 1711-1712.

14. Bugger H, Schwarzer M, Chen D, Schrepper A, Amorim PA, Schoepe M, Nguyen TD, Mohr FW, Khalimonchuk O, Weimer BC and Doenst T. (2010). Proteomic remodelling of mitochondrial oxidative pathways in pressure overload-induced heart failure. *Cardiovasc Res* **85**, 375-384.

15. Cha HN, Choi JH, Kim YW, Kim JY, Ahn MW and Park SY. (2010). Metformin inhibits isoproterenol-induced cardiac hypertrophy in mice. *Korean J Physiol Pharmacol* **14**, 377-384.

16. Chan AYM, Soltys CM, Yound ME, Proud CG and Dyck JRB. (2004). Activation of AMP-activated protein kinase inhibits protein synthesis associated with hypertrophy in the cardiac myocyte. *J Biol Chem* **279**, 32771-32779.

17. Chandler MP, Kerner J, Huang H, Vazquez E, Reszko A, Martini WZ, Hoppel CL, Imai M, Rastogi S, Sabbah HN and Stanley WC. (2004). Moderate severity heart failure does not involve a downregulation of myocardial fatty acid oxidation. *Am J Physiol Heart Circ Physiol* **287**, H1538-H1543.

18. Chen J, Chemaly ER, Liang LF, LaRocca TJ, Yaniz-Galende E and Hajjar RJ. (2011). A new model of congestive heart failure in rats. *Am J Physiol Heart Circ Physiol* **301**, H994-H1003.

19. Cittadini A, Napoli R, Monti MG, Rea D, Longobardi S, Netti PA, Walser M, Sama M, Aimaretti G, Isgaard J and Sacca L. (2012). Metformin prevents the development of chronic heart failure in the SHHF rat model. *Diabetes* **61**, 944-953.

20. Cohn JN Ferrari R and Sharpe N. (2000). Cardiac remodeling- concepts and clinical implications: a consensus paper from an international forum on cardiac remodeling. *J Am Coll Cardiol* **35**, 569-582.

21. Davel APC, Fukuda LE, Lima De Sa L, Munhoz CD, Scavone C, Sanz-Rosa D, Cachofeiro V, Lahera V and Rossini LV. (2008). Effects of isoproterenol treatment for 7 days on inflammatory mediators in the rat aorta. *Am J Physiol Heart Circ Physiol* **295**, H211-H219.

22. de las Fuentes L, Herrero P, Peterson LR, Kelly DP, Gropler RJ and Davila-Roman VG. (2003). Myocardial fatty acid metabolism: independent predictor of left ventricular mass in hypertensive heart disease. *Hypertension* **41**, 83-87.

23. Dhalla AK, Hill MF and Singal PK. (1996). Role of oxidative stress in transition of hypertrophy to heart failure. *J Am Coll Cardiol* **28**, 506-514.

24. Dunn ME, Manfredi TG, Cosmas AC, Vetter FJ, King JN and Rodgers RL. (2011). Mechanical function, glycolysis, and ultrastructure of perfused working mouse hearts following thoracic aortic constriction. *Cardiovasc Pathol* **20**, 343-351.

25. Dyck JRB and Lopaschuk GD. (2006). AMPK alterations in cardiac physiology and pathology: enemy or ally? *J Physiol* **574**, 95-112.

26. El-Mir MY, Nogueira V, Fontaine E, Averet N, Rigoulet M and Leverve X. (2000). Dimethylbiguanide inhibits cell respiration via an indirect effect targeted on the respiratory chain complex I. *J Biol Chem* **275**, 223-228.

27. Francis GS, Benedict C, Johnstone DE, Kirlin PC, Nicklas J, Liang C, Kubo S, Rudin-Toretsky E and Yusuf S. (1990). Comparison of neuroendocrine activation in patients with left ventricular dysfunction with and without congestive heart failure. *Circulation* **82**, 1724-1729.

28. Fukuta H and Little WC. (2007). Contribution of systolic and diastolic abnormalities to heart failure with a normal and a reduced ejection fraction. *Prog Cardiovasc Dis* **49**, 229-240.

29. Galindo CL, Skinner MA, Errami M, Olson LD, Watson DA, Li J, McCormick JF, McIver LJ, Kumar NM, Pham TQ and Garner HR (2009). Transcriptional profile of isoproterenol-induced cardiomyopathy and comparison to exercise-induced cardiac hypertrophy and human cardiac failure. *BMC Physiol* doi:10.1186/1472-6793-9-23.

30. Garnier A, Fortin C, Delomenie C, Momken I, Veksler V and Ventura-Clapier R. (2003). Depressed mitochondrial transcription factors and oxidative capacity in rat failing cardiac and skeletal muscles. *J Physiol* **551**, 491-501.

31. Gibbs M, Veliotes DGA, Anamourlis C, Badenhorst D, Osadchii O, Norton GR and Woodiwiss AJ. (2004). Chronic β-adrebireceptor activation increases cardiac cavity size through chamber remodeling and not via modifications in myocardial material properties. *Am J Physiol Heart Circ Physiol* ***287***, H2762-H2767.

32. Goffart S, von Kleist-Retzow JC and Wiesner RJ. (2004). Regulation of mitochondrial proliferation in the heart: power-plant failure contributes to cardiac failure in hypertrophy. *Cardiovasc Res* **64**, 198-207.

33. Grimm D, Elsner D, Schunkert H, Pfeifer M, Griese D, Bruckschlegel G, Muders F, Riegger GAJ and Kromer EP. (1998). Development of heart failure following isoproterenol administration in the rat: role of the rennin-angiotensin system. *Cardiovasc Res* **37**, 91-100.

34. Gundewar S, Calver JW, Jha S, Toedt-Pingel I, Ji SY, Nunez D, Ramachandran A, Anaya-Cisneros M, Tian R and Lefer DJ. (2009). Activation of AMP-activated protein kinase by metformin improves left ventricular function and survival in heart failure. *Circ Res* **104**, 403-411.

35. Hardie DG. (2003). Minireview: the AMP-activated protein kinase cascade: the key sensor of cellular energy status. *Endocrinology* **144**, 5179-5183.

36. Hardie and Carling. (1997). The AMP-activated protein kinase: Fuel gauge of the mammalian cell? *Eur J Biochem* **246**, 259-273.

37. Heather LC, Catchpole AF, Stuckey DJ, Cole MA, Carr CA and Clarke K. (2009). Isoproterenol induces *in vivo* functional and metabolic abnormalities; similar to those in the infracted rat heart. *J Physiol Pharmacol* **60**, 31-39.

38. Hill MF and Singal PK. (1996). Antioxidant and oxidative stress changes during heart failure subsequent to myocardial infarction in rats. *Am J Pathol* **148**, 291-300.

39. Hock MB and Kralli A. (2009). Transcriptional control of mitochondrial biogenesis and function. *Annu Rev Physiol* **71**, 177-203.

40. Huss JM and Kelly DP. (2005). Mitochondrial energy metabolism in heart failure: a question of balance. *J Clin Invest* **115**, 547-555.

41. Ide T, Tsutsui H, Kinugawa S, Utsumi H, Kang D, Hattori N, Uchida K, Arimura K, Egashira K and Takeshita A. (1999). Mitochondrial electron transport complex I is a potential source of oxygen free radicals in the failing myocardium. *Circ Res* **85**, 357-363.

42. Ide T, Tsutsui H, Hayashidani S, Kang D, Suematsu N, Nakamura K, Utsumi H, Hamasaki N and Takeshita A. (2001). Mitochondrial DNA damage and dysfunction associated with oxidative stress in failing hearts after myocardial infarction. *Circ Res* **88**, 529-535.

43. Iglewski M, Hill JA, Lavandero S and Rothermel BA. (2010). Mitochondrial fission and autophagy in the normal and diseased heart. *Curr Hypertens Rep* **12**, 418-425.

44. Kahn BB, Alquier T, Carling D and Hardie DG. (2005). AMP-activated protein kinase: ancient energy gauge provides clues to modern understanding of metabolism. *Cell Metab* **1**, 15-25.

45. Kato T, Niizuma S, Inuzuku Y, Kawashima T, Okuda J, Tamaki Y, Iwanaga Y, Narazaki M, Matsuda T, Soga T, Kita T, Kimura T and Shioi T. (2010). Analysis of metabolic remodelling in compensated left ventricular hypertrophy and heart failure. *Circ Heart Fail* **3**, 420-430.

46. Kelly DP and Scarpulla RC. (2004). Transcriptional regulatory circuits controlling mitochondrial biogenesis and function. *Genes Dev* **18**, 357-368.

47. Kemp CD and Conte JV. (2012). The pathophysiology of heart failure. *Cardiovasc Pathol* doi:10.1016/j.carpath.2011.11.007

48. Kim J, Wei Y and Sowers JR. (2008). Role of mitochondrial dysfunction in insulin resistance. *Circ Res* **102**, 401-414.

49. Kirpichnikov D, Mcfarlane SI and Sowers JR. (2002). Metformin: an update. *Ann Intern Med* **137**, 25-33.

50. Kola B, Boscaro M, Rutter GA, Grossman AB and Korbonits M. (2006). Expanding role of AMPK in endocrinology. *Trends Endocrinol Metab* **17**, 205-215.

51. Kralova E, Mokran T, Murin J and Stankovicova. (2008). Electrocardiography in two models of isoproterenol-induced left ventricular remodelling. *Physiol Res* **57**, 583-589.

52. Jullig M, Hickey AJ, Chai CC, Skea GL, Middleditch MJ, Cost S, Choong SY, Philips ARJ and Cooper GJ. (2008). Is the failing heart out of fuel or a worn engine running rich? A study of mitochondria in old spontaneously hypertensive rats. *Proteomics* **8**, 2556-2572.

53. Larkin JE, Frank BC, Gaspard RM, Duka I, Gavras H and Quackenbush J. (2004). Cardiac transcriptional response to acute and chronic angiotensin II treatments. *Physiol Genomics* **18**, 152-166.

54. Larsson N, Wang J, Wilhelmsson H, Oldfors A, Rustin P, Lewandoski M, Barsh GS and Clayton DA. (1998). Mitochondrial transcription factor A is necessary for mtDNA maintenance and embryogenesis in mice. *Nat Genet* **13**, 231-236.

55. Leenen FHH, White R and Yuan B. (2001). Isoproterenol-induced cardiac hypertrophy: role of circulatory versus cardiac rennin-angiotensin system. *Am J Physiol Heart Circ Physiol* **281**, H2410-H2416.

56. Leong HS, Grist M, Parsons H, Wambolt RB, Lopaschuk GD, Brownsey R and Allard MF. (2002). Accelerated rats of glycolysis in the hypertrophied heart: are they a methodological artefact? *Am J Physiol Endocrinol Metab* **282**, E1039-E1045.

57. Li H, Yin R, Chen D, Liu D, Wang D, yand Q and Dong Y. (2007). Long-term activation of adenosine attenuates monophosphate-activated protein kinase attenuates pressure-overload-induced cardiac hypertrophy. *J Cell Biochem* **100**, 1086-1099.

58. Lionetti V, Stanley WC and Recchia FA. (2011). Modulation fatty acid oxidation in heart failure. *Cardiovasc Res* **90**, 202-209.

59. Liu Z, Hilbelink DR, Crockett WB and Gerdes AM. (1991). Regional changes in hemodynamics and cardiac myocyte size in rats with arotocaval fistulas. 1. Developing and established hypertrophy. *Circ Res* **69**, 52-58.

60. Melenovsky V, Benes J, Skaroupkova P, Sedmera D, Strnad H, Kolar M, Vlcek C, Petrak J, Benes Jr J, Papousek F, Oliyarnyk O, Kazdova L and Cervenka L. (2011). Metabolic characterization of volume overload heart failure due to arortocaval fistula in rats. *Mol Cell Biochem* **354**, 83-96.

61. Messaoudi SE, Rongen GA, de Boer RA and Riksen NP (2011). The cardioprotective effects of metformin. *Curr Opin Lipidol* **22**, 445-453.

62. Mikusova A, Kralova E, Tylkova L, Novotova M and Stankovicova T. (2009). Myocardial remodelling induced by repeated low doses of isoproterenol. *Can J Physiol Pharmacol* **87**, 641-651.

63. Minotti G, Menna P, Salvatorelli E, Cairo G and Gianni L. (2004). Anthracyclines: Molecular advances and pharmacologic developments in antitumor activity and cardiotoxicity. *Pharmacol Rev* **56**, 185-229.

64. Murad N and Tucci PJF. (2000). Isoproterenol-induced hypertrophy may result in distinct left ventricular changes. *Clin Exp Pharmacol Physiol* **27**, 352-357.

65. Murray AJ, Edwards LM and Clarke K. (2007). Mitochondria and heart failure. *Curr Opin Clin Nutr Metab Care* **10**, 704-711.

66. Nagano M, Higaki J, Nakamura F, Higashimori K, Nagano N, Mikami H and Ogihara T. (1992). Role of cardiac angiotensin II in isoproterenol-induced left ventricular hypertrophy. *Hypertension* **19**, 708-712.

67. Nishio Y, Kanazawa A, Nagai Y, Inagaki H and Kashiwagi A. (2004). Regulation and role of the mitochondrial transcription factor in the diabetic rat heart. *Ann N Y Acad Sci* **1011**, 78-85.

68. Norton GR, Woodiwiss AJ, Gaasch WH, Mela T, Chung ES, Aurigemma GP and Meyer TE. (2002). Heart failure in pressure overload hypertrophy: the relative roles of ventricular remodelling and myocardial dysfunction. *J Am Coll Cardiol* **39**, 664-671.

69. Opie LH. (2004). The metabolic vicious cycle in heart failure. *Lancet* **364**, 1733-1734.

70. Opie LH and Knuuti J. (2009). The adrenergic-fatty acid load in heart failure. *J Am Coll Cardiol* **54**, 1637-1646.

71. Osadchii O, Norton G, Deftereos D, Muller D and Woodiwiss A. (2006). Impact of chronic β-adrenoceptor activation on neurotensin-induced myocardial effects in rats. *Eur J Pharmacol* **553**, 246-253.

72. Osadchii OE, Woodiwiss AJ, Deftereos D and Norton GR. (2007). Temporal changes in myocardial adrenergic regulation with teh progression to pump dysfunction after chronic β-adrenoreceptor activation in rats. *Eur J Physiol* **455**, 251-260.

73. Osadchii OE, Norton GR, McKechnie R, Deftereos D and Woodiwiss AJ. (2007). Cardiac dilatation and pump dysfunction without intrinsic myocardial systolic failure following chronic β-adrenoreceptor activation. *Am J Physiol Heart Circ Physiol* **292**, H1898-H1905.

74. Packer M. (1995). Evolution of the neurohormonal hypothesis to explain the progression of chronic heart failure. *Eur Heart J* **16**, 4-6.

75. Packer M. (1992). The neurohormonal hypothesis: a theory to explain the mechanism of disease progression in heart failure. *J Am Coll Cardiol* **20**, 248-254.

76. Packer M. (1988). Neurohormonal interactions and adaptations in congestive heart failure. *Circulation* **77**, 721-730.

77. Parati G and Esler M. (2012). The human sympathetic nervous system: its relevance in hypertension and heart failure. *Eur Heart J* **33**, 1058-1066.

78. Patten IS and Arany Z. (2011). PGC-1 coactivators in the cardiovascular system. *Trends Endocrinol Metab* doi:10.1016/j.tem.2011.09.007.

79. Recchia FA, McConnell PI, Bernstein RD, Vogel TR, Xu X and Hintze T. (1998). Reduced nitric oxide production and altered myocardial metabolism during the

decompensation of pacing-induced heart failure in the conscious dog. *Circ Res* **83**, 969-979.

80. Ren J, Pulakat L, Whaley-Connell and Sowers JR. (2010). Mitochondrial biogenesis in the metabolic syndrome and cardiovascular disease. *J Mol Med* **88**, 993-1001.

81. Rimbaud S, Sanchez H, Garnier A, Fortin D, Bigard X, Veksler V and Ventura-Clapier R. (2009). Stimulus specific changes of energy metabolism in hypertrophied heart. J Mol *Cell Cardiol* **26**, 952-959.

82. Robinson MM, Richards JC, Hickey MS, Moore DR, Phillips SM, Bell C and Miller BF. (2010). Acute β-adrenergic stimulation does not alter mitochondrial protein synthesis or markers of mitochondrial biogenesis in adult men. *Am J Physiol Regul Inter Comp Physiol* **298**, R25-R33.

83. Rosca MG and Hoppel CL. (2010). Mitochondrial in heart failure. *Cardiovasc Res* **88**, 40-50.

84. Russell LK, Finck BN and Kelly DP. (2005). Mouse models of mitochondrial dysfunction and heart failure. *J Mol Cell Cardiol* **38**, 81-91.

85. Sahn DJ and Henry WL. (1978). Clinical applications of real-time two-dimensional scanning in congenital heart disease. *Cardiovasc Clin* **9**, 295-316.

86. Sawyer DB and Colucci WS. (2000). Mitochondrial oxidative stress in heart failure: “oxygen wastage” revisited. *Circ Res* **96**, 119-120.

87. Schreiber SS, Oratz M, Evans C, Reef F, Klein I and Rothschild AM. (1973). Cardiac protein degradation in acute overload in vitro: reutilization of amino acids. *Am J Physiol* **224**, 338-345.

88. Shizukuda Y, Buttrick PM, Geenen DL, Borczuk AC, Kitsis RN and Sonnenblick EH. (1998). B-adrenergic stimulation causes cardiocyte apoptosis: influence of tachycardia and hypertrophy. *Am J Physiol Heart Circ Physiol* **275**, H961-H968.

89. Stanley WC and Chandler MP. (2002). Energy metabolism in the normal and failing heart: potential for therapeutic interventions. *Heart Fail Rev* **7**, 115-130.

90. Stewart S, Wilkinson D, Hansen C, Vaghela V, Mvungi R, McMurray J and Sliwa K. (2008). Predominance of heart failure in the heart of Soweto study cohort. *Circulation* **118**, 2360-2367.

91. Taegtmeyer H. (2004). Cardiac metabolism as a target for the treatment of heart failure. *Circulation* **110**, 894-896.

92. Taimor G, Schluter KD adn Piper Hm. (2001). Hypertrophy-associated gene induction after β-adrenergic stimulation in adult cardiomyocytes. *J Mol Cell Cardiol* **33**, 503-511.

93. Teerlink JR, Pfeffer JM adn Pfeffer MA. (1994). Progressive ventricular remodelin in response to diffuse isoproterenol-induced myocardial necrosis in rats. *Circ Res* **75**, 105-113.

94. Triposkiadis F, Karayannis G, Giamouzis G, Skoularigis J, Louridas G and Butler J. (2009). The sympathetic nervous system in heart failure. *J Am Coll Cardiol* **54**, 1747-1762.

95. Tsutsui H, Tsuchihashi-Makaya M, Kinugawa S, Goto D and Takeshita A. (2006). Clinical characteristics and outcome of hospitalized patients with heart failure in japan. *Circ J* **70**, 1617-1623.

96. Turdi S, Fan X, Li J, Zhao J, Huff AF, Du M and Ren J. (2010). AMP-activated proein kinase deficiency exacerbates aging-induced myocardial contractile dysfunction. *Aging Cell* **9**, 592-606.

97. Turer AT, Malloy CR, Newgard CB and Podgoreanu MV. (2010). Energetics and metabolism in the failing heart: important but poorly understood. *Curr Opin Clin Nutr Metab Care* **13**, 458-465.

98. Tuunanen H and Knuuti J. (2011). Metabolic remodelling in human heart failure. *Cardiovasc Res* **90**, 251-257.

99. van Bilsen M, van Nieuwenhoven FA and van der Vusse GJ. (2009). Metabolic remodelling of the failing heart: beneficial or detrimental? *Cardiovasc Res* **81**, 420-428.

100. Ventura-Clapier R, Garnier A and Veksler V. (2003). Energy metabolism in heart failure. *J Physiol* **555**, 1-13.

101. Ventura-Clapier R, Garnier A and Veksler V. (2008). Transcriptional control of mitochondrial biogenesis; the central role of PGC-1α. *Cardiovasc Res* **79**, 208-217.

102. Viollet B, Mounier R, Leclerc J, Yazigi A, Fortez M and Andreelli. (2007). Targeting AMP-activated protein kinase as anovel therapeutic approach for the treatment of metabolic disorders. *Diabetes Metab* **33**, 395-402.

103. Wang X, Zhang J, Li L, Zhao X, Tao H and Zhang L. (2011). Metformin improves cardiac function in rats via activation of AMP-activated protein kinase. *Clin Exp Pharmacol Physiol* **38**, 94-101.

104. Watson AMD, Hood SG and May CN. (2006). Mechanisms of sympathetic activation in heart failure. *Clin Exp Pharmacol Physiol* **33**, 1269-1274.

105. Wong ML and Medrano JF. (2005). Real-time PCR for mRNA quantification. *Biotechniques* **39**, 75-85.

106. Whittington HJ, Hall AR, McLaughlin AP, Hausenloy DJ, Yellon DM and Mocanu MM. (2012). Chronic metformin associated cardioprotection against infarction: not just a glucose lowering phenomenon. *Cardiovasc Drugs Ther* **27**, 5-16.

107. Woodiwiss AJ, Tsotestsi OJ, Sprott S, Lancaster EJ, Mela T, Chung ES, Meyer TE and Norton GR. (2001). Reduction in myocardial collagen cross-linking

parallels left ventricular dilatation in rat models of systolic chamber dysfunction. *Circulation* **103**, 155-160.

108. Wu Z, Puigserver P, Andersson U, Zhang C, Adelmant G, Mootha V, Troy A, Cinti S, Lowell B, Scarpulla RC and Spiegelman BM. (1999). Mechanisms controlling mitochondrial biogenesis and respiration through the thermogenic coactivator PGC-1. *Cell* **98**, 115-124.

109. Xie Z, Lau K, Eby B, Lozano P, He C, Pennington B, Li H, Rathi S, Dong Y, Tian R, Kem D and Zou MH. (2011). Improvement of cardiac functions by chronic metformin treatment is associated with enhanced cardiac autophagy in diabetic OVE26 mice *Diabetes* **60**, 1770-1778.

110. Yin M, van der Horst ICC, van Melle JP, Qian C, van Gilst WH, Sillje HHW and de Boer RA. (2011). Metformin improves cardiac function in a nondiabetic rat model of post-MI heart failure. *Am J Physiol Heart Circ Physiol* **301**, H459-H468.

111. Yin FCP, Spurgeon HA, Rakusan K, Weisfeldt ML and Lakatta EG. (1982). Use of tibial length to quantify cardiac hypertrophy: application in the aging rat. *Am J Physiol Heart Circ Physiol* **12**, H941-H942.

112. Zarrinpashneh E, Beauloye C, Ginion A, Pouleur A, Havaux X, hue L, Viollet B, Vanoverschelde J and Bertrand L. (2008). AMPKα2 counteracts the development of cardiac hypertrophy induced by isoproterenol. *Biochem Bioph Res Co* **376**, 677-681.

113. Zhou G, Myers R, Li Y, Chen Y, Shen X, Fenyk-Melody J, Wu M, Ventre J, Doebber T, Fujii N, Musi N, Hirshman MF, Goodyear LJ and Moller DE. (2001). Role of AMP-activated protein kinase in mechanism of metformin action. *J Clin Invest* **108**, 1167-1174.